Experimental Study of Laser-Induced Forward Transfer of non-Newtonian Fluids

Susen Lösch

Master Thesis
Stockholm, Sweden 2020

Abstract

Laser-Induced Forward Transfer (LIFT) can be used to print different kinds of materials on to a receiver with a higher resolution than common printing technologies used in the microelectronics industry. This technology could enable the production of ever smaller devices and the development of diminutive sensors and device components. The method is very precise and can be used to apply solder paste, as well. Solder paste is used to form solder joints between a circuit board and surface mounted components. The smallest solder paste droplets produced today are ≈ 200 μm in diameter.

In this thesis, single solder particles (10-25 μm) were successfully transferred from type 5 solder paste by a single femtosecond laser pulse. Depending on objective magnification, the laser wavelength and the spreading method, the threshold pulse energy was between 110 and 2000 nJ. This part of the study showed that the transfer of very small particles is possible and that the resolution of this method is mainly limited by the size of the transferred particle, not by the process itself.

The measurements indicate that the necessary energy to transfer a particle increases with the size of the particle. The necessary energy increases approximately with 6,2 nJ per micrometer diameter. Depending on the amount of flux above or underneath the particle the necessary energy to transfer a particle might differ. It is supposed that the method of preparing the paste layer influences the distribution of flux around the solder particles.

Successful transfer of clean droplets between 40 and 260 μm could be shown for a type 6 and a type 9 solder paste, as well. The transfer is mainly influenced by the gap width, the paste viscosity, the layer thickness and the pulse energy. Different combinations of these variables lead to three transfer modes, which are called ”droplet”, ”zero” and ”explosion”. The variables also affect the size of the droplet.

The droplet mode is the only transfer to produce clean deposits.

In this mode the laser radiation causes the solvents to evaporate and bend the paste layer sufficiently to touch the receiver. When the donor is removed, the droplet is formed on the receiver.

The gap width is the most critical variable. It needs to be smaller than 5 μm to transfer droplets and only a small variation of some micrometers can change the transfer mode. The viscosity of the paste needs to be adjusted very carefully to reach the droplet mode and to match further work steps. Decreasing the solder mass fraction by only one percent will increase the droplet diameter by approx. 11 μm. A solder mass fraction over 87 % leads to explosion transfers.

Droplets could be produced for a layer thickness between 15 and 40 μm. The thicker the layer, the larger the resulting droplet. The impact of layer thickness on the droplet diameter decreases with 0,51 μm per μm thickness per percent of increasing solder mass fraction. If the layer thickness is over 40 μm zero transfers can occur. A layer thinner than 23 μm is prone to explosion transfers.

An increasing laser power increases the probability of droplet production. At the maximum available power of 2 W, approx. 70 % of all pulses produced a droplet.

Sammanfattning

Laser-Induced Forward Transfer (LIFT) används för att applicera olika typer av material på en mottagare med en högre upplösning än med teknologier som vanligtvis används i mikroelektronikindustrin. Tekniken möjliggör produktion av allt mindre enheter och utveckling av mindre sensorer och enhetskomponenter. Metoden är mycket noggrann och kan även användas för att applicera lödpasta. Lödpasta används till lödningar mellan ett kretskort och ytmonterade komponenter. De minsta dropparna av lödpasta som produceras idag är ca 200 μm i diameter.

I detta examensarbete överfördes enskilda lödpartiklar med storleken 10-25 μm framgångsrikt från typ 5 lödpasta med en enda femtosekunds laserpuls. Beroende på objektivets förstoring, laservåglängden och spridningsmetoden var pulsens tröskelenergi mellan 110 och 2000 nJ. Denna del av studien visade att överföring av mycket små partiklar är möjlig och att upplösningen av denna metod är huvudsakligen begränsad av storleken på de överförda partiklarna, inte av metoden i sig.

Mätningarna indikerar att tröskelenergin som behövs för att överföra en partikel ökar med partikelns storlek. Den nödvändiga energin ökar med 6,2 nJ per mikrometer diameter ungefär. Beroende på mängden av flussmedel över eller under partikeln, skiljer sig den nödvändiga energin för att överföra en partikel. Det antas att sättet att sprida lödpastan påverkar distribution av flussmedel runt lödpartiklarna.

Framgångsrik överföring av rena droppar mellan 40 och 260 μm kunde också visas för lödpasta av typ 6 och typ 9. Överföringen påverkas huvudsakligen av avståndet mellan lagret av lödpasta och mottagaren, lödpastans viskositet, lagrets tjocklek och pulsenergin. Olika kombinationer av dessa variabler leder till tre överföringslägen, som kallas ”droplet”, ”zero” och ”explosion”. De nämnda variablerna orsakar också storleksvariation av den överförda droppen.

Droplet-läget är den enda överföringen som producerar rena drop-

par. I detta läge orsakar laserstrålningen att lösningsmedlen förångas och böjer pastaskiktet tillräckligt för att kunna beröra mottagaren. När givaren med lagret av lödpasta tas bort bildas droppen på mottagaren.

Avståndet mellan pastalagret och mottagaren är den mest kritiska variabeln. Det måste vara mindre än 5 μm för att överföra droppar och endast en liten förändring på någon mikrometer kan ändra överföringsläget. Viskositeten hos pastan måste justeras mycket noggrant för att nå droppläget och för att passa in i kommande steg i arbetsprocessen. Att minska andelen lödpartiklar med endast en procent kommer att öka droppdiametern med 11 μm. En andel av lödpartiklar över 87 % leder till explosionöverföringar.

Droppar kan produceras från lagren som är mellan 15 och 40 μm tjocka. Ju tjockare lagret är, desto större blir den resulterande droppen. Om lödpartikelandelen ökas med en procent minskas påverkan av lagrets tjocklek på droppdiametern med 0,51 μm per μm tjocklek. Zero-överföringar förekommer om lagertjockleken är över 40 μm. Ett lager som är tunnare än 23 μm är benäget för explosionsöverföringar. En ökande lasereffekt ökar sannolikheten för droppproduktion. Med den maximala tillgängliga effekten på 2 W uppnåddes en droppandel på 70 %.

Acknowledgements

I would like to thank PhD Gustaf Mårtensson for giving me the opportunity to work on this project, introducing me to the topic, uncomplicatedly providing paste samples and objectives and sharing his expertise on the topic.

An additional special thanks to my supervisors at MST at KTH Simone Pagliano and PhD Miku Laakso for their help in the lab and taking their time to discuss ideas and problems.

I would also like to thank the whole MST group for their help with the laser work station, other lab equipment and mostly for making me feel welcome.

Special thanks to Iris Lüke for her feedback on English spelling and grammar.

Finally, I would like to thank Lars-Gunnar Andersson and Prof. Fredrik Laurell for accepting me as a master thesis student, their feedback and their flexibility regarding the finishing of the project.

Contents

1 Introduction

1.1 Overview of Laser-Induced Forward Transfer - LIFT - processes

The microelectronics industry aims to bring ever smaller devices to the market. A major challenge, especially in the production of medical devices, is the development of diminutive sensors and device components [10], and the precise fitting of surface mounted components on circuit boards. One technology to overcome the prevailing problems and limits is Laser-Induced Forward Transfer (LIFT).

LIFT is a technology used to print different kinds of materials directly on to a receiver. This method is very precise and can be used for example, to apply solder paste, as shown in this thesis. This paste is used to connect electrical components to pads on circuit boards and needs to be deposited with great precision.

The first efforts to apply LIFT for different purposes were performed in 1969/1970 [1, 2], but it was not further investigated until 1986, when Bohandy et al. used an excimer laser to deposit copper patterns on silicon substrates [3]. Since then, many different LIFT based technologies, such as Laser Induced Backward Transfer (LIBT), Matrix Assisted Pulsed Laser Evaporation-Direct Write (MAPLE-DW), Laser-Induced Thermal Imaging (LITI), Laser Molecular Implantation (LMI), Ballistic Laser Assisted Solid Transfer (BLAST), Blister-Actuated LIFT (BA-LIFT), Film-Free Laser Printing (FF-LIFT), Laser Decal Transfer (LDT) and Congruent LIFT have been developed [4].

A basic LIFT setup as shown in figure 1.1 consists of a thin donor layer or film of metal, ink, paste or semiconductors and biomolecules placed on a transparent carrier, as well as a receiver substrate and a pulsed laser. The laser is focused on the interface of the carrier and the donor layer. A short, single laser pulse is used to heat up a defined area of the donor material, leading to vaporization. This causes sudden gas expansion, which induces pressure onto the material and propels a small amount of donor material towards the re-

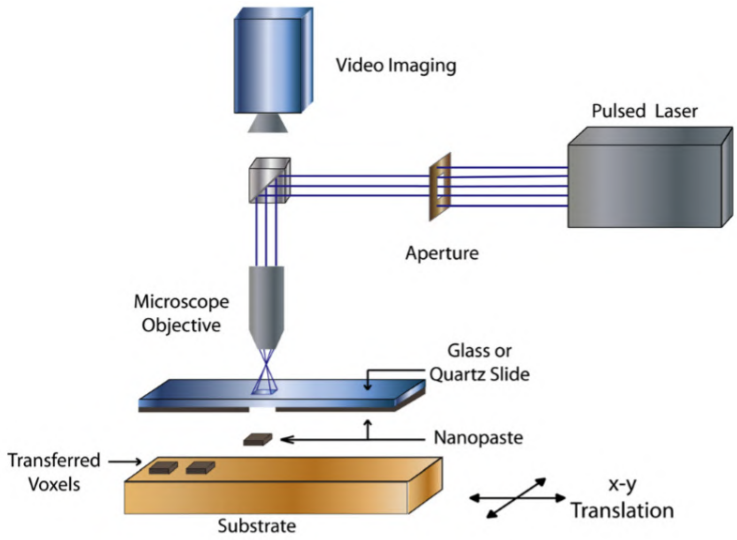

Fig. 1.1: Schematic illustrating the basic elements of a LIFT system showing transfer of nanopaste [6].

ceiver through an air gap of up to 100 μm width [4]. The transfer process differs depending on the properties of the donor material.

For solid metals the laser radiation causes a small volume of the donor layer to melt and material at the carrier-donor interface to vaporize. Gas expansion pushes the molten material towards the receiver.

Other solid or liquid materials, which are sensitive to high temperatures, like biomaterials, can be transferred using a dynamic release layer (DRL). The most common DRL is the photodecomposing triazene polymer (TP), a polymer containing aryl-triazene chromophores with high absorption at several common wavelengths. This allows the use of common excimer lasers like Nd:YAG (266 nm and 355 nm) and XeCL (308 nm). The transfer of solids is particularly difficult, because the transferred particles tend to break, through strong

acting forces during detachment from the donor and through impact on the receiving substrate.

Liquids usually produce a jet of material when transferred by LIFT. The jet travels across the air gap and hits the receiver forming a droplet. The droplet keeps growing until the jet breaks up.

High-viscosity (90-150 Pa·s) suspensions, e.g. silver-nanopaste, are of particular interest for LIFT. Their viscoelastic properties open up the possibility to transfer exact shaped voxels (congruent LIFT). During the process no bubbles or shock waves occur. Therefore, the risk for destruction of the voxel during the separation from the donor layer is very low. Furthermore, the travel speed of the voxel across the air gap is much lower than that of other materials, so when hitting the receiver the forces on the voxel are orders of magnitude smaller preventing the voxel to splatter or break [6].

LIFT offers some essential advantages for the printing of solder paste compared to established printing methods like jet printing, stencil printing, screen printing or solder jetting. First of all, LIFT is a nozzle and mask free and contactless technology. Hence no clogging of a nozzle like in the case of jet printing occurs. No expensive and complicated handling of masks is required like in screen or stencil printing, and the risk of damaging sensitive parts of the board is reduced. Furthermore, it offers the possibility to transfer different materials within a wide range of viscosities ($\approx$ 0,01 Pa·s to more than 100 Pa·s). Also the resolution is enhanced as a smaller deposit size of solder paste ($\approx$ 45 μm) is reached compared to commonly used techniques (215 μm for jet printing). This makes it a highly flexible process, which is especially suitable for prototyping and complex production series. The LIFT technology is also promising to provide high production speeds when required by using a laser beam scanner. A further important advantage is the possibility to print in 3D [7, 8].

1.2 Aims of this thesis

The goal of this thesis is to develop a method to transfer single dots of solder paste with a constant diameter below 200 μm with the help of a femtosecond (fs) laser. Such a method has the benefit to reduce thermal effects and its collateral damages [11]. LIFT with a fs-laser has been performed successfully for solid metals and transparent polymer films [12, 13, 14].

To understand the behaviour of the solder paste during the LIFT process, rheological properties, like viscosity and thixotropy, are investigated in detail. The quality of the transferred voxels are correlated to these properties.

In 2015 Mathew et al. showed for the first time that the transfer of solder paste with a nanosecond laser is possible [5]. Furthermore, the transfer of high-viscosity silver pastes, which have similar viscosity as solder pastes with small solder spheres, have been studied in detail. [9].

2 Theory

2.1 Rheology and Non-Newtonian fluids

Rheology is the science of deformation and flow of matter [15]. It is used to describe the flow behaviour of complex fluids like polymers, suspensions, pastes and other liquids, also called non-Newtonian fluids. Rheology defines certain standard flows to create measurable and comparable values for different materials. Shear flow (see fig. 2.1), for example, is regularly used to estimate the viscosity of a fluid.

Newtonian fluids exhibit a constant viscosity and follow Newton's law of viscosity:

$$\tau = \mu \frac{dv}{dy}$$

where τ is the shear stress, μ is the viscosity and $\frac{dv}{dy}$ is the shear rate. In comparison, non-Newtonian fluids have varying viscosity which depends on the shear rate, ultimately leading to a range of flow behaviours. These behaviours are described by rheological properties.

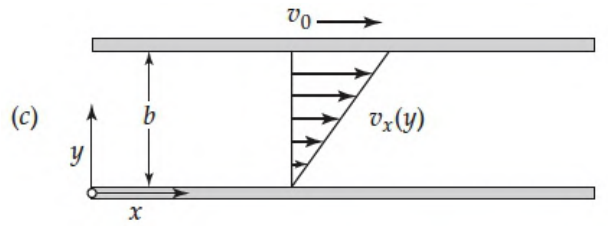

Fig. 2.1: Schematic of generation of simple shear flow [24].

2.1.1 Rheological properties

Rheology defines several different parameters and properties of viscous materials. The property with most influence on flow behaviour is viscosity, which is defined as "the ratio of the shear stress to the shear rate in a simple shear flow" [16] as shown in Newton's law of viscosity. It is given in units of $[\mathrm{Pa} \cdot \mathrm{s}]$. Viscosity describes the internal friction or resistance of a liquid to flow. Non-Newtonian fluids exhibit a changing viscosity under the impact of shear. When increasing the shear rate, the viscosity may increase or decrease non-linearly. This is called shear-thinning or shear-thickening respectively, where shear-thinning is the most common. It needs to be considered, when the used fluid is exposed to shear forces, for example, when the material is pushed through a narrow tube.

Some fluids "flow only when stresses are above a threshold stress" [15], which is called yield stress in rheology. When the stress is increased above the yield stress, the material deforms. Once the stress is removed from a Newtonian fluid, the deformation will stop instantly, while non-Newtonian fluids will deform on its own even after

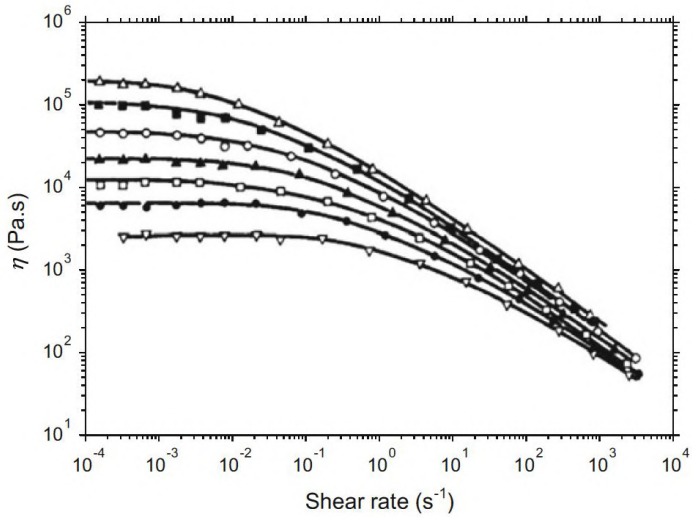

Fig. 2.2: Non-Newtonian fluids commonly show a decreasing viscosity under increasing shear rate. This property is called shear-thinning. The graph shows the viscosity of a low density polyethylene melt at different temperatures. Top curve, T = 388 K, bottom curve T = 513 K [16].

the stress has been removed as the molecular structure of these fluids sustains stress for a period of time, the so called relaxation time.

The microstructure of a material and the time it takes to change it determines the thixotropy of a material. The word thixotropy combines the greek words thixis (stirring or shaking) and trepo (turning or changing) [25]. Microstructures can be composed of particles, fibres, drops or polymers, which are distributed, aligned or entangled. During stirring or shearing flow stresses occur, which break down the microstructure of the material. This leads to a decrease of viscosity, as in shear-thinning. At rest the microstructure reassembles into the initial state and viscosity increases again. The main difference between shear-thinning and thixotropy is the timescale. Shear-thinning means an instant decrease of viscosity as the shear rate changes. Thixotropy

relates to breakdown processes occurring over seconds or hours. Rebuilding of the microstructure usually takes significantly longer than its breakdown. Barnes [25] describes thixotropy as the ”reversible decrease of materials viscosity with time under constant shear rate or shear stress, followed by a gradual recovery of the structure after the removal of the shear stress or rate”. For some gel-like materials the resulting change in viscosity can cause them to become fully liquid during stirring and then solidify after some time at rest, this is called extremely shear-thinning.

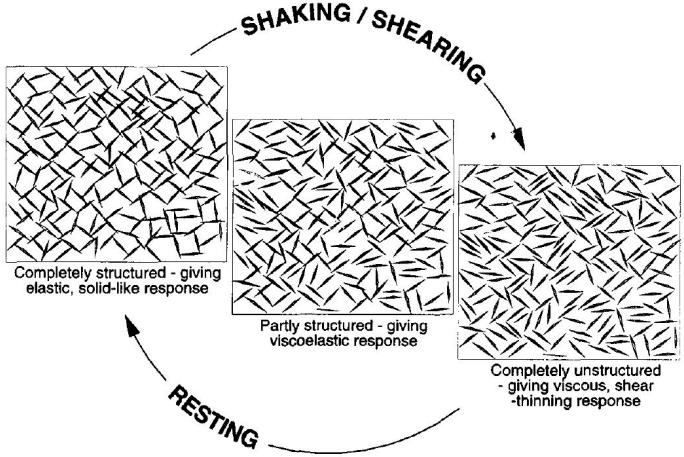

Fig. 2.3: Breakdown of a 3D thixotropic structure based on Barnes [25].

The processes described by thixotropy are the reason why many non-Newtonian fluids show a hysteresis, when observing viscosity under changing shear rate or stress. By increasing the shear rate shear thinning occurs. When the shear rate is decreased again, the viscosity over shear rate will not follow the same curve. Instead it shows a lower viscosity for the same shear rate, because rebuilding microstructures to their initial state is a slow process and produces a hysteresis curve.

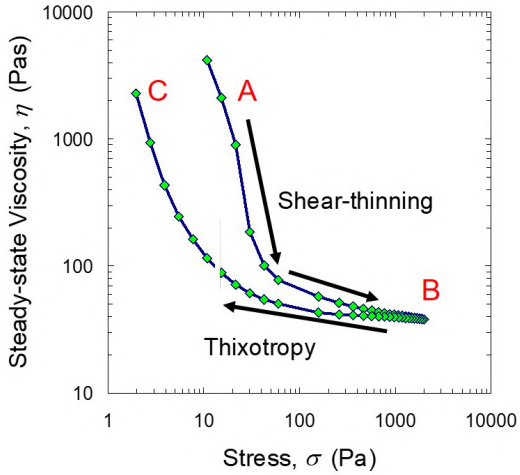

Fig. 2.4: Thixotropic behaviour of a non-Newtonian material. The graph shows the hysteresis of viscosity over shear rate or stress [26].

Figure 2.4 shows that the initial viscosity (point A) will be reached again, but only after a certain length of time after the microstructure is fully rebuilt. This can take minutes or even hours, depending on the material.

2.1.2 Constitutive equation and material functions of fluids

The mathematical description of rheological properties of fluids relates the applied force or stress to the resulting deformation as a function of time.

For non-Newtonian fluids the functions of kinematic parameters that characterize their rheological behaviour are called rheological material functions. These functions can be derived from the laws of conservation of mass and linear momentum, which govern isothermal deformation. From the conservation of mass an equation for the mass balance, the so called continuity equation, can be derived, as

$$\text{Continuity equation: } 0 = \frac{\partial \rho}{\partial t} + \nabla \cdot (\rho \underline{v})$$

From the conservation of linear momentum the microscopic momentum equation for general fluids, which is called the equation of motion, can be derived as

$$\text{Equation of motion: } \rho(\frac{\partial \underline{v}}{\partial t} + \underline{v} \cdot \nabla \underline{v}) = -\nabla \cdot \underline{\underline{\Pi}} + \rho \underline{g}$$

with the material density ρ, the local velocity $\underline{v}$, the total stress tensor $\underline{\underline{\Pi}}$, which contains the information about the state of stress at a point, and the gravity field $\underline{g}$.

The thermodynamic pressure p and the deformation of the fluid are the major contributions to the total stress tensor $\underline{\underline{\Pi}}$. Other factors influencing $\underline{\underline{\Pi}}$ that are not produced by thermodynamic pressure are summarized in the so called extra stress tensor $\underline{\underline{\tau}}$. It includes the stress produced by fluid deformation and depends strongly on the type of fluid. A formula that describes $\underline{\underline{\tau}}$ is called the stress constitutive equation. Rheology aims to define appropriate stress constitutive equations for non-Newtonian fluid. These formulas express the molecular stresses generated in the flow in terms of kinetic variables, such as velocities, strains, and derivatives of velocities and strains. Once a suitable constitutive equation is defined, it can be inserted into the equation for $\underline{\underline{\Pi}}$ and subsequently into the equation of motion. Solving the equation of motion and the continuity equation results in the velocity field or other flow variables.

It is known that non-Newtonian fluids have different material properties than Newtonian fluids. Therefore $\underline{\underline{\tau}}$ needs to include not only information about velocities, strains, and derivatives of velocities and strains, but also material information, which makes the constitutive equation of non-Newtonian fluids a much more complicated function than for Newtonian fluids. The material information "is contained in the density ρ, in the format of the constitutive equation, and in material-based information contained in the unknown constitutive equation."[15]

The constitutive equation of a non-Newtonian fluid is more complicated to find, than for a Newtonian fluid, mainly because the form of the constitutive equation is unknown. Experiments under standard flow conditions are performed to find so called rheological material functions. Standard flows are defined flow situations to measure functions of time, strain or strain rate, which depend on the structure of the material, and to make experiment results comparable. For non-Newtonian fluids a wide variety of material properties are functions of kinematic parameters, instead of constants as for Newtonian fluids. These functions are material functions and characterize the rheological behaviour of non-Newtonian fluids [15].

2.2 Solder paste

2.2.1 Content and usage

Solder paste is used to connect electrical components to pads on circuit boards. It is a very dense suspension of a flux and solder powder in the form of small metal alloy spheres. The alloy spheres make up 80-90 % of the mass of the paste, but due to its high density only 40-50 % of the volume. The spheres have a diameter of 2 to 150 μm, depending on the type (see table 2.1).

Originally, tin-lead (Sn-Pb) alloys were used, but for health reasons lead-free alloys, like tin silver copper (Sn/Ag/Cu (SAC)) and tin/antimony (Sn/Sb) were introduced. In this master thesis SAC alloys are used. These consist of mainly tin mixed with approximately 3 % silver and 0,5 % copper. Spheres offer a high volume to surface ratio, which keeps oxidation within a limit. Typically, solder powder is produced by gas atomisation or centrifugal atomisation [29].

The flux includes several chemicals, which influence viscosity, slump, thixotropic index and other rheological properties (see sec. 2.2.3). The constituents of flux are a flux base or filmogen ($\approx$ 35-45 % by weight), solvents ($\approx$ 30-50 %), activators ($\approx$ 0,5-5 %) and thixotropic agents ($\approx$ 5-8 %) [28].

The flux base needs to be fluid at soldering temperatures (200-250 °C) and to have good heat transfer properties. The main function of the flux base is to dissolve the present surface metal oxides and act as an oxygen barrier by coating the hot metal surface during reflow (see sec. 2.2.5). Furthermore, it reduces the surface tension of the molten solder. This promotes the wetting of the metal pad by molten solder and ensures a good electrical connection [29].

Mostly, the flux base alone is not sufficient to guarantee good wetting. Therefore activators, typical halides, like dimethyl or diethyl ammonium chloride, are added. They are used to remove the oxide-film of the solder powder and decrease the wetting time, but also increase corrosivity. To avoid increased corrosivity, organics with carboxyl- or amine-groups are commonly used today. These organics only reach a mild level of activation, which is common in electronic applications.

Thixotropic agents like castor oil, beeswax and carnauba wax and aliphatic amide [28, 29] are used to increase the viscosity and to modify the thixotropic behaviour of the paste. This is essential for stencil printing to ensure proper detachment of the mask and for jet printing to guarantee a constant flow through the syringe.

Solvents need to follow special demands to guarantee proper soldering. Solvents support the paste application and must have a low evaporation rate during the storage and printing process, but need to evaporate during the reflow process. Commonly used solvents are different ethers and forms of ethanol and other alcohols.

2.2.2 Classification

Solder pastes can be classified by the size range of the alloy spheres (see table 2.1) or by the flux base.

There are two commonly used flux bases: rosin and water-soluble bases. Rosin is a complex mixture of high molecular weight acidic molecules including abietic and pimaric type acids [27]. It is a natural product from various pine tree species making it is easily avail-

Table 2.1: Types of solder paste. At least 80 % of the solder spheres in the paste are in the given range of size [17, 18].

Type	Particle size in μm
9	1-5
8	2-8
7	2-11
6	5-15
5	10-25
4	20-38
3	25-45
2	45-75
1	75-150

able. As its chemical composition is subjected to natural variation and not well defined, many solder paste manufactures produce synthetic rosin and resins and use a mixture of these to create pastes suitable for different applications.

Water-soluble fluxes consist of organic materials in a solution of strong activators. During reflow, strong activators generate residues, which can damage the circuit. Therefore, the residues need to be washed away. For water-soluble fluxes this can be performed with water.

2.2.3 Rheological properties of solder paste

The rheological properties of solder paste have a large influence on the correct placement of solder paste and the precise positioning of components. Generally, a solder paste should exhibit fine particles, high viscosity, high yield stress (low slump) and be strongly shear-thinning, conversely thixotropy is not desirable [48]. Different applications require different properties, so the rheological characteristics

need to be quantified and comparable. Therefore, there are standards, e.g. the Japanese industrial standard Z 3284, which describes in detail how to quantify rheological properties of solder paste.

Solder paste is a non-Newtonian fluid that exhibits a complex flow behaviour, which is typically described by the parameters in the following headers:

Viscosity

The viscosity of solder paste is commonly 30-300 Pa·s, but changes substantially with shear rate and temperature (see fig. 2.5.).

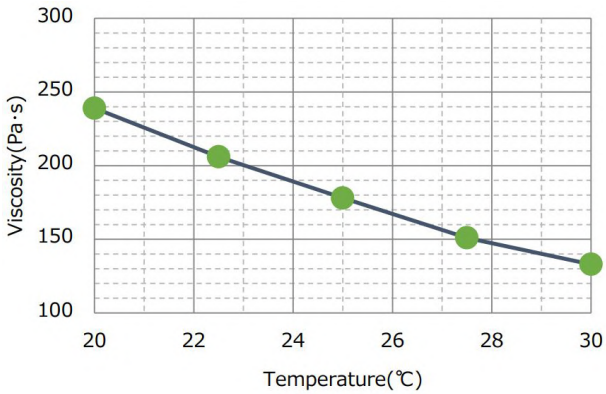

Fig. 2.5: Viscosity over temperature for a lead free solder paste (TLF-401-11) [37].

Solder paste shows shear-thinning behaviour under the impact of shear force. This is especially important in stencil and jet printing to enable the paste to be pressed through the mask aperture or the narrow tube.

The viscosity of solder paste is affected by the flux composition, the metal content and the particle size distribution [19]. A higher metal content and decreased mean solder powder particle size increase the viscosity [23, 41], because they increase the internal friction in the

paste. To reach appropriate values, thinners can be added [23].

A larger particle size distribution decreases viscosity [23]. Because it may be more difficult for the material to build up a complete microstructure. Instead, it is always at least partly unstructured, resulting in a decreased viscosity (see fig. 2.3).

Also, the flux composition influences the viscosity. The kind and the proportion of flux base, solvent and thixotropic agents determine the viscosity of the flux and consequently the viscosity of the solder paste. Different flux bases have different softening points, influencing the viscosity-temperature relation. Generally solvents with higher molecular weight increase the viscosity of the paste [20].

Thixotropic index

Most solder pastes are also thixotropic. Therefore, it is necessary to consider the shear history of the paste, when aiming for a certain value of viscosity. The thixotropic index is defined as [41]:

$$TI = log_{10} \frac{\eta(\tau_A)}{\eta(\tau_B)}$$

with the viscosity at defined stress or shear rate $\eta(\tau_A)$ and $\eta(\tau_B)$ and the ratio of applied stress $\frac{\tau_A}{\tau_B} = 0,1$. A typical thixotropic index is between 0,5 and 0,7 [32, 37, 40, 47]. This means the viscosity changes with a factor of 3 to 5 for the applied stress values. The thixotropic index is misleading because it quantifies the ”strength” of the materials shear-thinning effect, but not the recovery of the microstructure. This confusing term dates back to the early days of rheology, when scientist did not strictly differ between shear-thinning and thixotropy. The thixotropic index is influenced by the kind of solvent and the thixotropic agents [20]. Pastes with high metal content and less viscous flux show low thixotropy. Furthermore, thixotropy is less pronounced in pastes containing spherical particles, because the inner 3D-structure can not change by rotation of the particles [25]. This leads to a more consistent rheological behaviour of the paste generally [23]. For example, a paste with spherical particles shows a more

stable viscosity during a workday, which makes it more suitable for solder printing [23].

Slump

Slump means the paste's tendency to spread after placement, which may cause bridging between printed pads [46]. Bridging is highly undesirable, because it leads to short circuits on the board. The slump describes the paste's ability to stay in one place as long as the yield stress is not exceeded. The yield stress is the point at which the solder paste changes from a solid-like to a liquid-like behaviour [49].

The slump is measured by printing standard patterns, which include pads with different, but defined distances. The samples are left at different temperatures, e.g. room temperature and 150 $^{\circ}C$ for a defined time and investigated under a light microscope. As a low slump is desired, the smallest gap still visible is determined. Typical values are below 0,7 mm under heat [50].

The fast rebuilding of the microstructure after shear-thinning ensures that the shape of the placed paste is retained and slumping is decreased [20].

A higher softening point of the flux base and a higher volatility of solvents at high temperature increase the viscosity of solder paste at high temperature, which contributes to less slump during heating [50]. Higher metal loadings tend to reduce slumping during reflow as well [23].

Tackiness

Tackiness describes the ability of the paste to hold a component in position. This property ensures the stable adhesion of the component during the process. It is quantified by pressing a probe of certain size with a well defined force into the paste and measuring the force it takes to release the probe from the paste. Usually a tackiness of more than 1 N is desired [37].

Due to the evaporation of solvents, the tackiness decreases when

the paste is exposed to the atmosphere [46]. High metal content decreases tackiness as well. On the other hand, this decreases slumping and those two properties need to be well balanced for a high quality-paste [41].

2.2.4 Mathematical description of the flow behaviour

The flow behaviour of a non-Newtonian fluid can be described by a constitutive equation or material functions, as mentioned above (sec. 2.1.2). Many solder pastes are described by the Herschel-Bulkley model [19, 21]:

$$\tau = \tau_0 + k_1 \dot{\gamma}^{n_1}$$

with the shear stress τ, the yield stress τ_0, the consistency index of the material k, the power law or flow index n_1 and the shear rate $\dot{\gamma} = \frac{\partial v}{\partial t}$. The Herschel-Bulkley model is a generalized Newtonian fluid model, which means that this constitutive equation is a generalized form of Newton's law of viscosity.

An easier model often applied, showing a similar precision is the Power law model [22]:

$$\tau = k_2 \dot{\gamma}^{n_2}$$

2.2.5 Reflow process

After the placement of the solder paste on the pads of the circuit board and the surface mounting of the components, the whole circuit board is heated under controlled conditions in a reflow oven to produce the actual solder joint. Conventional infrared (IR) reflow, forced air convection reflow and vapour phase reflow are the most common reflow methods. IR ovens are generally not suited for lead-free reflow soldering, because they can not guarantee thermal equilibrium across the board [39].

The heating itself follows a specific temperature over time profile (see figure2.6), which depends on the kind and size of the components on the board, the solder paste composition and the reflow

method. There are two different profiles: the ramp profile and the soak profile. For forced air convection reflow, a linear ramp profile is more adequate [38]. In vapour phase reflow the ramp profile can be used, because the method itself provides extremely good thermal equilibrium [29]. Furthermore, overheating is not possible in vapour phase reflow. The soak profile is used for IR reflow because it can lower the temperature gradient across board components.

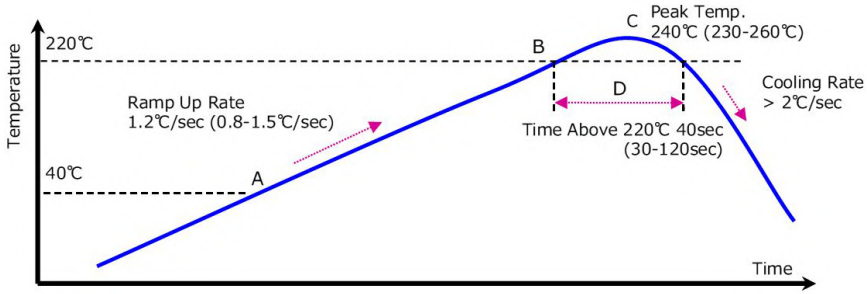

Fig. 2.6: During reflow the actual solder joint is produced. The figure shows the ramp reflow profile of M705-ULT369 solder paste [37].

The ramp profile is structured into three stages:

1. ”Heating” Stage

The temperature is raised continuously to 200 °C during 60 to 120 s with a maximum temperature gradient of 0,8 - 1,5 °C/s to prevent slumping of the paste and breaking of sensitive components. This leads to the evaporation of the solvent and softening of rosins and thixotropic agents. ”The solvent evaporation rate may vary significantly from paste to paste, depending on the solvent type used” [38]. For example, ethanol has a boiling point of $\approx$ 80 °C, while commonly used ethers evaporate at 200 to 230 °C. Generally, the softening point of solder paste is $\approx$ 100 °C.

If the temperature is raised too quickly, the solid flux components will soften, while large parts of the solvent have not evaporated yet. This would make the paste very liquid and it would tend to high

slumping. [29]

”Most fluxes are activated at temperatures above 150 °C” [38]. The flux base and the activators eliminate surface oxide films from the solder powder particles. Furthermore, the flux becomes more liquid, surrounds the solder powder particles and prevents re-oxidation. The solvents evaporate nearly completely.

2. Reflow Stage

The board is heated to the peak temperature (220 to 260 °C) with a temperature gradient of 1 to 4 °C/s, so that solder particles melt. Exposed to temperatures well above the melting point (217 to 220 °C), solder flows and the actual soldering occurs. The system has to stay at that temperature for 30 to 120 s to secure complete melting of all solder particles and proper wetting. An excessive time above 200 °C or too high peak temperature can lead to the destruction of the circuit board material and low quality solder joints.

3. Cooling Stage

At the end, the board gradually cools down to room temperature with a temperature gradient of 2 to 4 °C/s and solder joints solidify. A fast cooling down provides improved solder joint quality, but too fast cooling can lead to component damages [39].

The soak profile is structured into four stages. The main difference to the ramp profile is a pre-heat and a soak stage instead of the heating stage. In the pre-heat stage the temperature rises from room to soak temperature (ca. 150 to 170 °C) by maximum 1 to 4 °C/s. In the soak stage the temperature slowly rises ($\approx$ 0,4 °C/s) to ca. 180 °C. At the end of that stage the heat should be uniformly distributed over the whole circuit. The reflow stage and cooling stage are similar to the ramp profile.

2.3 Introduction to femtosecond lasers and their advantages

Femtosecond (fs) lasers emit light pulses in the femtosecond range (1fs $= 1 \cdot 10^{-15}$ s). Many fs lasers are diode-pumped, solid-state lasers with Nd:YAG or Yb:YAG crystals as a gain medium, which emit light in the visible or near-infrared spectrum. Often the light pulses are generated by passive mode locking followed by chirped pulse amplification. For passive mode locking a saturable absorber is inserted in the laser cavity. It absorbs low-intensity radiation, but transmits light above a certain threshold. The chirped pulse amplification setup increases the power of the outgoing laser pulse. High power fs lasers can emit light with up to 1500 W average power [43].

The total energy and power in a single pulse are:

$$E_{pulse} = \frac{P_{avg}}{f}$$

$$P_{pulse} = \frac{E_{pulse}}{t_{pulse}}$$

with the average power of the laser radiation P_{avg}, the pulse frequency f and the duration of one pulse t_{pulse}.

The high illumination intensity of fs laser pulses can cause multiphoton absorption. That means strongly focused fs laser pulses can be absorbed by transparent materials, which do not usually absorb the applied wavelength.

After fs laser radiation it takes a few hundred fs to a few ps for the electrons to reach thermal equilibrium. This is shorter than the time to transfer energy from the electrons to the atom lattice, which is 1 to 100 ps and depends on the electron-photon strength. Therefore, most of the photon energy causes electron heating, while the lattice mainly stays unaffected. "Only a very small fraction of the laser pulse energy is transformed to heat" [45] and material might be ablated before heat conduction can occur. This minimizes the heat-affected

zone (HAZ) compared to laser applications with longer pulses [42, 44]. This main advantage of fs lasers compared to other lasers is widely used in eye surgery and microfabrication, where the process is also called ”cold ablation”.

2.4 Energy estimation of LIFT of solder paste droplets

LIFT of solder paste follows the same procedure as many other LIFT applications (see ch. 1), but a few essential differences in the physical processes need to be considered. The paste itself is quite sticky (see tackiness in sec. 2.2.3) and to detach a small volume from a paste layer, this stickiness needs to be overcome. The energy for this process is provided by the laser radiation. It is used to evaporate the solvents and produce a force by gas expansion, which pushes some material away from the layer towards the receiver.

Solder flux is optically transparent in a wide range of the visible and infrared spectrum. Common solvents are ethanol and different ethers, which are also transparent to visible light.

Therefore, most of the laser radiation and its energy will just transmit the flux and eventually be absorbed by solder balls in the radiated region. There is no data about the reflectance or absorbance of SAC solder yet. To overcome this limitation the reflectance of the pure metals included in SAC solder is taken as an approximation. The greatest part of SAC solder is tin, which has a reflectance of $\approx 0,8$ over the whole visible and near infrared spectrum [51]. Hence, approximately 80 % of the incoming energy E_{in} is lost by reflection.

If the wavelength of the laser photons matches the excitation energy of the atoms in the solder ball, photon energy will be absorbed and converted into thermal energy E_{therm} by electron excitation and stepwise relaxation.

$$E_{therm} = 0,2E_{in} \tag{1}$$

To assume how much of the incoming energy is deposited in the evaporated solvent, the necessary thermal energy to heat up the sol-

der and the flux base and to evaporate the solvent needs to be compared. Generally for the heating of a liquid or a solid below its melting or boiling point, the required energy is defined as:

$$E_{heat} = m \cdot c_p \cdot \Delta T$$

with the mass of the material m, the isobaric specific heat constant c_p and the temperature difference between room temperature and boiling point ΔT. The energy necessary for the heating and evaporation of the solvent is defined as:

$$E_s = m \cdot (c_p \cdot \Delta T + c_V) \tag{2}$$

where c_V is the heat of vaporization. It is assumed that heating and evaporation occurs under nearly isobaric conditions. The specific heat constant changes with temperature, but for convenience a constant specific heat constant is assumed.

Table 2.2: Comparison of mass fraction and thermal constants of solder paste contents.

	SAC solder [54]	Solvent (ethanol) [52]	Flux base (rosin) [55]
Approx. mass fraction in the paste	$\frac{8}{9}$	$\frac{1}{18}$	$\frac{1}{18}$
Specific heat capacity $[\frac{J}{kg \cdot K}]$	223	2570	1300
Heat of vaporization $[\frac{J}{kg}]$	-	$919 * 10^3$	-
Fraction of thermal energy	15,7 %	78,6 %	5,7 %

Based on the data in table 2.2, E_s is:

$$E_s = 0,786 \cdot E_{therm} \tag{3}$$

If the amount of thermal energy is sufficient, the solvent will evaporate leading to sudden gas expansion. This induces pressure

on to the surrounding paste and eventually moves it away from the place of evaporation.

The force produced by evaporation can be derived from the ideal gas law defined as:

$$\begin{aligned} p \cdot V_{gas} &= m \cdot R_s \cdot T \\ p &= \frac{m \cdot R_s \cdot T}{V_{gas}} \\ \frac{F_{gas}}{A} &= \frac{m \cdot R_s \cdot T}{V_{gas}} \\ F_{gas} &= \frac{m \cdot R_s \cdot T \cdot A}{V_{gas}} \end{aligned}$$

with the specific gas constant R_s ($180 \frac{\mathrm{J}}{\mathrm{kg \cdot K}}$ for ethanol), the absolute temperature T, the volume V_{gas} and the area A, which F_{gas} acts on.

This force is produced by the evaporation and gas expansion of flux solvents and acts on a certain area A of the voxel. There are two forces that act against the force produced by gas expansion. One is the adhesive force F_{sticky} of the paste and the other is the force F_o of the atmospheric pressure $p_o = 101,3$ kPa on the same area: $F_o = A \cdot p_o$. To successfully use LIFT, the force produced by gas expansion needs to be greater than the sum of the forces acting against it.

$$F_{gas} \geq F_{sticky} + F_o$$

The tackiness (see 2.2.3) is a measure of the adhesive forces of the paste and shows how much force is necessary to separate a part of the paste. Typically tackiness of solder paste is 1 to 1,5 N for a defined probe area.

Using the probe radius r_{probe}, it is possible to calculate a tack pressure: $p_{tack} = \frac{F_{tack}}{\pi \cdot {r_{probe}}^2}$. To estimate the force necessary to detach a part of the paste, the area A_{sticky}, where the parts were initially connected, need to be calculated. For the transfer of a voxel A_{sticky} can be simply

described as the side area of the voxel in the donor layer. For a circular laser spot (with top hat beam configuration) this is a cylinder side approximately. The radius of the assumed cylinder equals the laser spot size radius r.

$$A_{sticky} = \pi \cdot 2r \cdot x$$

with the paste layer thickness x. So

$$\begin{aligned} F_{sticky} &= A_{sticky} \cdot p_{tack} \\ &= \pi \cdot 2r \cdot x \cdot \frac{F_{tack}}{\pi \cdot {r_{probe}}^2} \end{aligned}$$

Calculating p_{tack} from typical values shows that $p_{tack} \ll p_o$. Furthermore, the areas where p_o and p_{tack} are applied, have similar size: $\pi \cdot r^2 \approx \pi \cdot 2r \cdot x$. So it is reasonable to assume:

$$\begin{aligned} F_{gas} &\geq F_o \\ \frac{m \cdot R_s \cdot T \cdot A}{V_{gas}} &\geq A \cdot p_o \\ \frac{m \cdot R_s \cdot T}{V_{gas}} &\geq p_o \end{aligned}$$

Assuming that solvents are just evaporated in the focal spot and that the heat affected zone has the shape of a cylinder, the volume is defined as $V_{gas} = \pi \cdot r^2 \cdot h$. Where h is the theoretical height of the gas cylinder. So

$$\begin{aligned} \frac{m \cdot R_s \cdot T}{\pi \cdot r^2 \cdot h} &\geq p_o \\ m &\geq p_o \frac{\pi \cdot r^2 \cdot h}{R_s \cdot T} \end{aligned}$$

Inserting this into the equation 2 and using a reasonable value for h the necessary energy to transfer a voxel of a certain size can be estimated as follow:

$$E_s \geq p_o \frac{\pi \cdot r^2 \cdot h}{R_s \cdot T} \cdot (c_p \cdot \Delta T + c_V) \tag{4}$$

It seems surprising, that the thickness of the paste layer does not influence the necessary energy to transfer a voxel. Therefore it is assumed, that $h \propto x$. That means, to be able to propel forward a thicker voxel of the same radius, a larger gas volume and thereby a greater h (r = const.) is needed. As $E_s \propto h$, this will lead to a greater threshold energy.

2.5 Previous methods of LIFT of solder paste

A group of scientists at the Naval Research Laboratory in Washington successfully transferred solder paste voxels in 2015 [5]. They used a nanosecond laser with a wavelength of 355 nm and a tophat beam profile. They produced voxels with a diameter of 45 μm using a Type 7 solder paste (see sec. 2.2.2), a silver release layer (150-250 nm thickness) and a donor layer thickness of 18 to 20 μm. Further successful experiments of LIFT of solder paste are not known.

A material that is quite similar to solder paste is silver nanopaste, which has been used successfully in LIFT by several research groups. Silver nanopaste is made of silver particles with a size in the nanometre range dispersed in a matrix of organic binders. The viscosity of nanopaste is similar to that of solder paste, but the metal particles are approximately 100 to 1000 times smaller. Therefore it is possible to transfer thinner layers of some micrometers and smaller voxels of nanopaste. Even successful 3D printing using the LIFT process has been reported [7, 8].

To reach a better resolution for LIFT of solder paste, smaller metal particles should be used. On the other hand, smaller particles will increase the metal surface and thereby the oxide content, which leads to solder joints of lower quality. More flux base and activators could be added to avoid oxidation, but this would decrease the viscosity, which will lead to undesired higher slump and lower tackiness.

In summary, the properties of the paste need to be well balanced between the different requirements. Therefore, it is difficult to define the best combination of components for a solder paste used in a LIFT

process. One task of this master thesis project is to identify suitable material properties for a successful LIFT process. Until now there has been no special LIFT-solder paste on the market, so solder paste for jet printing is used instead.

3 Problem definition

The aim of this thesis is to develop a method to transfer single droplets of solder paste with the help of a femtosecond laser. The droplets shall have a diameter smaller than 200 μm, a circular shape and not fragmented or splattered. In the industry these drops will be reflowed into solder joints of surface mounted components on circuit boards. The smallest solder paste droplets produced today are $\approx$ 200 μm. Producing smaller droplets will save material and space. Hence, electrical devices and sensors can be fabricated even smaller. The use of the fs laser has the potential to reduce thermal effects and their collateral damages [9]. Furthermore, the limited HAZ of a fs-laser supports the production of smaller droplets, than with a picosecond or nanosecond laser.

At first, the transfer of single solder balls will be investigated. The goal is to find the ideal wavelength and threshold power for two different paste types (type 5 and type 6, see sec. 2.2.2). If successful, this part of the study will show that the transfer of very small particles ($\approx$ 5 μm) is possible and that the resolution of this method is mainly limited by the size of the transferred particle, not by the method in itself.

Secondly, deposits with a diameter smaller than 200 μm shall be produced. The deposits should not show any splatter or debris, when the ideal paste thickness, gap width, laser spot size and power are applied. If successful, this part of the thesis work will open up for a method of placing electrical connections on circuit boards with higher resolution than any other method used today.

4 Design of experiments

4.1 LIFT of single solder particles

4.1.1 Sample preparation

A glass slide with a thin layer of solder paste serves as the donor for this experiment. The glass slide, which is used as the carrier, is a common cover slide of thickness 0 ($\approx$ 90 μm). The solder paste is spread with a scraper as thin as possible to isolate balls. A quality check is routinely performed by light microscopy to investigate if the isolation rate is sufficient. Some balls still stick together, due to the nature of the flux. Applied pastes were "M705-LFAC19 Senju Metal Industry Co", a type 5 paste and the type 6 paste "Alpha JP-500".

An approximately 0,5x6x6 mm large silicon chip is used as a receiver. The chip is covered with a thin layer of "JP500T6" flux from "MacDermid Alpha®" or double-sided tape ($\approx$ 30 μm) to prevent transferred balls from hopping or rolling off the receiver. The chip is placed in an $\approx$ 600 μm deep rectangular cavity on an aluminium plate with the flux covered side facing upward (see fig. 4.1).

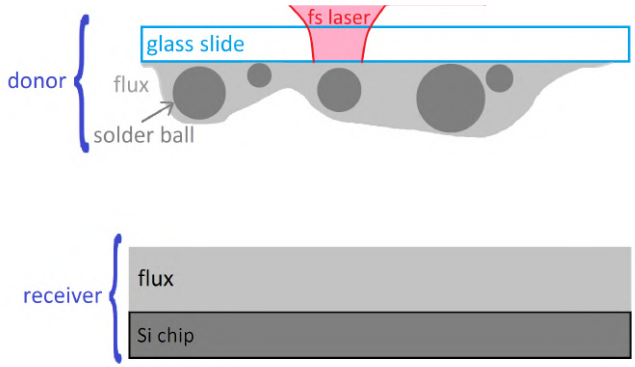

Fig. 4.1: Design for LIFT of single solder balls.

4.1.2 Assembly for the LIFT process

The aluminium (Al) plate is mounted onto the moveable stage of the laser workstation. ”Olympus Plan N” objectives with 10x and 4x magnification are used to focus the laser beam. The laser used for all experiments was a ”Spirit® femtosecond laser 1040-4-SHG”, which offers wavelengths of 1040 nm and 520 nm. The laser beam and the camera are focused on the surface of the Si chip and the chip is marked with 1 mm spaced position crosses to identify transferred particles later. The donor is placed on top of the hole on the Al plate with the paste facing down. The depth of the hole in the metal plate determines the gap width between donor and receiver, which is commonly between 40 and 130 μm.

To bring the interface of the paste layer and the glass slide into the focus of the laser and the camera, the height of the stage is adjusted. Furthermore, the stage is moved horizontally to direct the laser beam on isolated solder balls. The pulse picker divider and the exposure duration are chosen to generate a single laser pulse onto the solder ball.

The goal is to find the threshold power for balls of different sizes. Therefore the power is increased from 1 mW, until small balls are transferred. Then the power is increased further to transfer medium and large particles. The applied power, the size and the coordinates of the solder ball are noted to generate a map of all laser shots.

4.1.3 Light microscope analysis

A ”Nikon optiphot” microscope was used to examine the Si chip with the transferred particles. The diameter and the coordinates of the transferred balls were measured to produce a similar map as for the laser shots. By comparing both maps the position of the balls can be verified and successful transfers can be identified. The data is analysed to define the energy necessary to transfer a single ball of a certain size.

4.2 LIFT of solder paste droplets

4.2.1 Sample preparation

To produce paste layers of different thicknesses on the same sample a glass wafer with three wet etched wells of varying depths is used (see fig.4.2). The glass wafer is approximately 700 μm thick and the wells are between 15 and 50 μm deep and approximately 1x0.5 cm large. The paste is spread into the wells with the long edge of a microscope slide covered with clear adhesive tape. The tape is used to reduce the unevenness in the paste layer. A second glass wafer with an etched well of 5 μm depth is used as a receiver.

The same type 6 paste as before is used. Additionally, a type 9 paste is mixed from "5N Plus SAC305" solder powder and "alpha®JP500T6" flux. The type 9 paste and a silver nanoparticle ink for screen printing from "Sigma-Aldrich" is used for this experiment as well. For this experiment no flux layer on the receiving Si chip is needed, because the amount of transferred flux is sufficient to hold the deposits in place on the receiver.

4.2.2 Assembly for the LIFT process

The same laser workstation and Al plate used for the LIFT of single particles are used. The used objective is a "Leica Germany PL Fluotar" with 2,5x magnification. For this set of experiments a wavelength of 1040 nm was used, because the laser workstation provides higher pulse energies at this wavelength.

The receiver is placed on the Al plate with the well facing upwards. The workstation provides a vacuum system, which is used to hold the receiver in place. The donor is placed on top of the receiver with the paste facing downward as shown in figure 4.2 and the laser is focused on the interface of paste and glass wafer.

The sample is parted into trials. These trials are divided into lines, which are illuminated with different laser powers (see fig. 4.3).

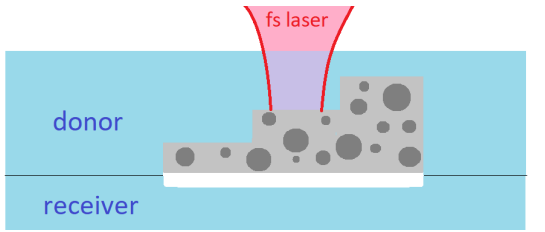

Fig. 4.2: Design for LIFT of solder paste droplets.

One line includes up to 100 equal pulses to gain data for statistical analysis. The repeatability of the trails was checked by having several lines of the same laser power on one sample.

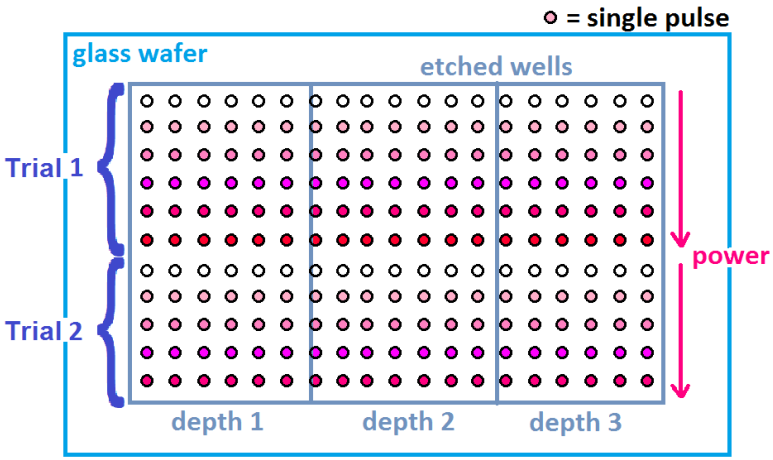

Fig. 4.3: Schematic of single pulse distribution over the sample. One row of pulses has equal laser power. The power is increased from row to row in each trial, which is shown by the different colours in the circles.

To transfer voxels of different diameters the stage is moved, so that the focus is 0-300 μm above the interface. This defocusing increases the laser spot size and thereby the size of the voxel. By vary-

ing both, the laser power and the laser spot size the best conditions for the transfer of droplets for every layer thickness can be found.

To avoid damaging the sample, the donor is removed by suction using a vacuum tube.

4.2.3 Analysis

The properties of the transferred droplets are investigated with the same microscope as for the single particle LIFT. First, it is checked if the transferred material shows splatter or debris. These are highly undesirable conditions. The material needs to form a clean droplet, to produce a high quality solder joint. The whole sample is imaged with the camera of the microscope. The resulting images are analysed using a MATLAB code to measure the drop diameters.

Also the donor is investigated under the microscope. The laser pulses leave marks on the paste layer, whose form gives information about the transfer mode (see ch. 6).

5 Limitations of the setup

5.1 LIFT of single solder balls

The setup followed mainly the design presented in section 4.1, but some parts of the experiment showed some unexpected aspects.

It could be observed that the way the paste is spread on the glass slide affects the threshold power. Probably, depending on the spreading method, the force with which the solder balls are pressed into the flux, varies. Furthermore the amount of flux surrounding the solder balls can be affected by the spreading method. This might influence the threshold power for the transfer of single balls.

Tests without a thin layer of flux or double-sided tape on the receiver showed that transferred particles appear far away from any laser shot or are lost. In contrast, with a flux layer for a maximum of

89 shots, all but three balls were found on the receiver, and could be related to a laser shot. It is reasonable to assume that the amount of transferred flux together with the particle is insufficient to attach the particle to the receiver.

Furthermore, it could be observed that the coordinates of the laser shot and the related found solder ball on the receiver did not match exactly. An average deviation of up to 60 μm, depending on the gap width between donor and receiver, was measured. The greater the gap width, the greater was the average deviation. It is supposed that this has two reasons. Firstly, if the laser is not directed onto the top of the solder ball. If the laser radiation does not hit the top accurately, there is a force pushing the ball sideways and not only forward, leading to the observed deviation. To focus exactly onto the top a higher magnification of the objective is necessary. Secondly, the flux around the particle might be unevenly distributed. This induces forces, which move the particle sideways, as well.

Measurements of the Al stage showed, that the holes in the plate are not perfectly parallel to the top of the stage. Instead, the area, where the Si chip is placed, is tilted. This leads to a variation of the gap width of $\approx$ 10 μm across the whole chip.

One aspect, which made it complicated to execute exact measurements was the low magnification of the used objectives. Firstly, it was only possible to differentiate between three rough ball sizes (small $\approx$ 10-15 μm, medium $\approx$ 15-20 μm, large $\approx$ 20-25 μm). Secondly, the 4x objective did not allow to distinguish between a single ball, a small pile of balls or just a contamination that stuck to the flux during the experiment, when using the type 5 solder paste. Due to these limitations, the type 6 solder paste with even smaller particles was not tested. All results relating the size of the balls and the threshold power are just approximate. This problem can be avoided with a paste including solder particles of just one size. Unfortunately these are not available on the market and it was decided to not continue the investigations.

5.2 LIFT of solder paste droplets

The setup of this experiment followed the planned design introduced in section 4.2.

The laser threshold power was measured for different thicknesses of solder paste layers. It was observed, that it is difficult to produce a smooth layer with the explained method. As the paste is very sticky, some solder particles attach to the edge of the tape covered glass slide while spreading the paste. This leaves an uneven paste layer on the receiver. Different types of tape were tested and the clear tape produced the smoothest layer. Due to the explained effect, the layer has an average height difference of an average ball diameter (see fig. 5.1). For voxels with small diameter and thickness, this might influence the threshold power and the form of transferred material significantly.

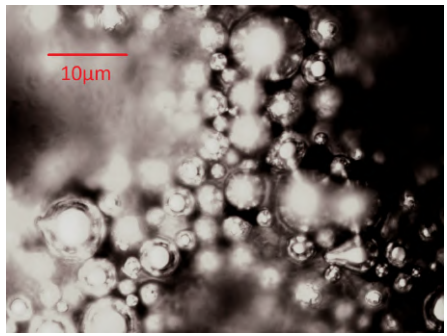

Fig. 5.1: Light microscope photo of a solder paste layer (type 6). The focus is on the particles (shiny circles) on the top of the layer. Obviously, there are areas, which are not in focus. The particles in these areas there are laying below the focal plane. The reason for this is, that some balls tend to stick to the squeegee during the spreading of the paste, leaving an uneven paste layer.

For solder paste it is very important to keep a gap width smaller than 5 μm to produce clean droplets as observed in initial tests.

Therefore a glass wafer without a well is used as a receiver to produce a minimum gap. This causes difficulties in the production of the samples. As explained the paste layer can be uneven. When placing the donor with the paste layer on the 0 μm-receiver, some areas of the layer might stick to the receiver and the sample becomes unusable. To avoid this the sample is built together before placing it in the laser workstation. If only small areas (estimated < 5 %) glued together the sample is considered as good. The glued areas are an indicator for a very small gap width. If large areas (> 5 %) of the sample are glued together the receiver is removed and a new layer is freshly spread. The receiver is cleaned and the sample is assembled again.

As the used laser beam is not perfectly Gaussian, it is impossible to vary the laser spot size by moving the whole setup out of focus (defocusing). Instead, the x and y-direction of the laser have different focal points causing an elliptical beam shape. Depending if the donor is closer to the focal point of the x or the y-direction, the shorter axis of the ellipse will be in x or y-direction, respectively. If the donor is placed in the middle between the focal points of x and y-direction, the laser spot will be circular, because there both directions are equally unfocused (see fig. 5.2).

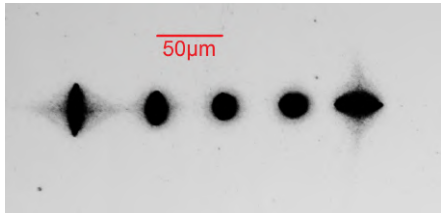

Fig. 5.2: Laser spot on Si chip after 8ms exposure at 1000 mW, 1040 nm and 100 kHz. From left to right the defocus is -400 μm, -100 μm, 0 μm, +100 μm, +400 μm.

A circular laser spot produces the most even energy distribution in the laser spot, which leads to a higher probability of producing

clean droplets. The explained problem can be circumvented by using different objectives to generate different sized circular spots. By focusing on a 250 nm layer of chromium it could be shown that a 2.5x objective produces a hole in the layer of maximum 38 μm diameter using the highest internal available power of 4 W. Lower laser powers produce a beam with a smaller spot size. A 4x objective produces a hole of 25,5 μm diameter at 4 W (see fig. 9.7 in appendix). The diameter of a type 6 solder particle is 5-15 μm. To guarantee that a sufficient amount of particles is fully exposed to the laser radiation and transferred even at lower laser powers, all experiments are performed with a 2.5x objective. For the type 9 and the nanopaste using a 4x objective would be sufficient, because the particles are smaller.

The focusing process meant to find at which distance the laser spot is circular. Using the nanopaste, the shape of the laser spot appeared clearly on the paste layer and the distance between the objective and the paste layer could be adjusted easily to focus the laser beam on the interface of paste layer and glass slide. When using one of the solder pastes, the form of the laser spot was not observable, because the larger particles scatter the imaging light more strongly. When glass slides of the same thickness are used, the focus should be in the same place regardless of which paste is used. Consequentially the same objective-paste layer distance can be used for all samples.

Standard settings are applied to the laser system to reach a single pulse. The internal pulse frequency is 100 kHz and the pulse picker divider was set to 1000, which leads to an external frequency of 100 Hz. Setting the duration of the opening of the shutter to 10 ms produces a single pulse. During initial tests, it could be observed that some randomly distributed laser shots transfer more material than most other shots. Additionally, when illuminating a chromium layer, some laser shots produced larger holes in the chromium layer than most other shots with the same power. It is supposed that two pulses in one shot cause this. In an extreme case a pulse can be released in the beginning and at the end of the 10 ms period the shutter is open

and two pulses expose the same area during one shot. To avoid this, the duration of the opening of the shutter was decreased to 9 ms.

6 Results

6.1 LIFT of single solder balls

Single solder particles were successfully transferred from type 5 solder paste using different magnifications and laser wavelengths. Two examples of transferred solder spheres are shown in figure 9.1 in the appendix. In initial experiments the solder paste was smeared out on the glass slide with a small plastic spatula. To calculate threshold pulse energies shown in table 6.1, the internal laser power was converted into the output power with data from figure 9.4 and 9.5 in the appendix.

Table 6.1: Threshold pulse energies for different magnifications and wavelengths for the smallest particles in the solder paste. The paste was smeared out with plastic spatula.

Objective magnification	10x	10x	4x
Laser wavelength in nm	520	1040	1040
Internal laser power in mW	50-55	2-10	110-180
Threshold pulse energy in nJ	110-120	250-270	600-800

The analysis of the experiment with an objective magnification of 10x and a laser wavelength of 520 nm indicates that the necessary energy to transfer a particle increases with the size of the particle (see fig.6.1). The necessary energy increases approximately with 6.2 nJ per micrometer diameter.

In the experiment with the 10x objective and 1040 nm wavelength balls could be transferred even with the lowest available en-

Fig. 6.1: Pulse energy over solder sphere diameter of successful transfers of single solder particles.

ergy of 250 nJ (see table 6.1). It is assumed that the threshold might be below the minimum energy available. The threshold for the 4x objective is approximately 450 nJ larger than for the 10x objective at 1040 nm. Using the 4x objective leads to a wider laser energy distribution and a lower peak energy. To reach the same peak energy as with the 10x objective, the total pulse energy needs to be significantly increased. All these values are only approximates as the threshold energy can vary considerably. It is supposed that the variation is caused by the uneven distribution of flux around the solder particles. Depending on the amount of flux above or underneath the particle the necessary energy to transfer a particle can differ.

In another experiment the paste was spread by scratching the tape covered edge of a microscope slide across the paste layer. Measurements of the threshold power showed higher variation (see table 6.2). Therefore it is supposed that the method used for spreading the paste influences the distribution of flux around the solder particles. Probably, using a plastic spatula leads to less flux around the particles, which leads to a lower threshold energy. Furthermore, the flux

is distributed more evenly, which results in a lower variation of the threshold energy than if the paste is spread with a microscope slide.

Table 6.2: Threshold pulse energies for different magnifications and wavelengths for the smallest particles in the solder paste. The paste was spread with the tape covered edge of a microscope slide.

Objective magnification	10x	4x
Laser wavelength in nm	1040	1040
Internal laser power in mW	10-40	200-500
Tthreshold pulse energy in nJ	270-340	850-2000

It could be successfully shown that small particles can be transferred one by one. As mentioned in section 5.1, the assumption about the flux behaviour made here could be easily proved with a paste including particles of only one size. This approach could be attempted in the future.

6.2 LIFT of solder paste droplets

6.2.1 Transfer modes

For all three available pastes successful transfers of clean droplets could be produced, but the conditions for a successful transfer vary between the pastes. This variation is caused by the different properties of the pastes (see table 6.3).
The given viscosity is temperature and shear-rate dependent. If the viscosity needs to be changed at constant temperature, the solder particle/flux mass ratio can be varied. Increasing the flux fraction by adding some flux to the paste will decrease the viscosity of the paste. Therefore the solder particle/flux is used as an indicator of a paste's viscosity.

The transfer is mainly influenced by four parameters: the gap width, the paste viscosity, the layer thickness and the laser power. Dif-

Table 6.3: Types of available Solder Paste and their properties [33, 34, 35, 36].

Paste type	Type 6	Type 9	Nanopaste
Particle size in μm	5-15	1-4	<1
Solder particle/flux mass ratio	87/13	$\approx$ 80/20 to 87/13	$\approx$ 55/45
Viscosity in Pa·s	20-300	unknown	4,8-10

ferent combinations of these variables lead to three transfer modes called ”droplet”, ”zero” and ”explosion”, respectively. These names refer to the form of the transferred material (see fig. 6.2).

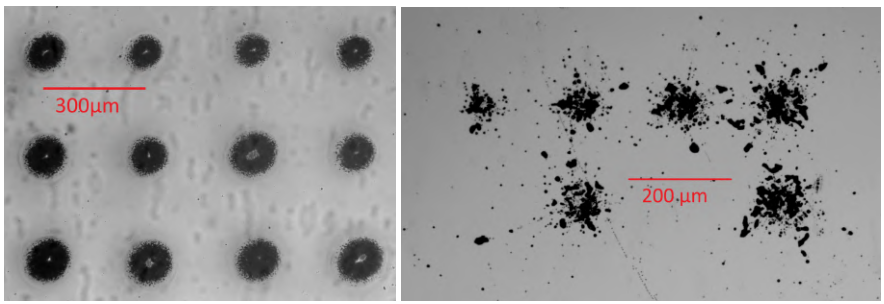

(a) Example of transferred material of droplet mode.

(b) Example of transferred material of explosion mode.

Fig. 6.2: Light microscope photo of transferred material of a Type 9 paste with a solder particle mass fraction of (a) $\approx$ 80 % and (b) $>$ 87 %.

Furthermore, each of these modes produces different marks in the paste layer, which provide information about the detachment processes during the transfer modes.

Droplet Mode
To deposit a clean droplet, the variables need to be in certain ranges to bend the paste layer and produce a hill of paste. This hill needs to overcome the gap width and touch the receiver. The actual droplet is produced by carefully lifting the donor away from the receiver as shown in figure 6.3.

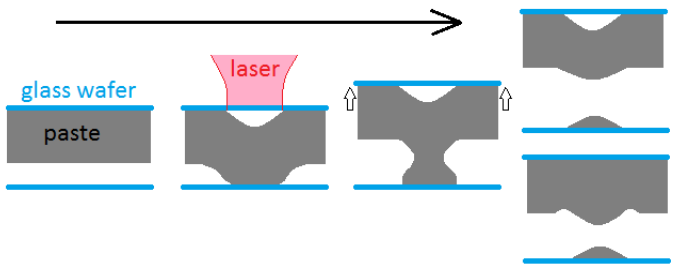

Fig. 6.3: Schematic of droplet mode transfer.

The droplet diameter and height are influenced by all parameters, but generally the height is several times smaller than the diameter. The highest measured droplet of type 6 solder paste was 40 μm high and had a diameter of 235 μm.

The lifting process can leave a mark on the donor. It can be either a hill or a hill with a ditch around (see fig. 6.4a). The hills can be up to $\approx$ 25 μm high and the ditches up to $\approx$ 10 μm deep. It is assumed that the formation of a hill or a hill with a ditch depends on gas leakage during the removal of the donor.
It was observed that the size of these marks decreased over a time period of some hours. Directly after application the paste is still fluid, but after some time the paste dries out and viscosity increases. Therefore the marks will never completely vanish, but they are most distinct directly after the LIFT process.

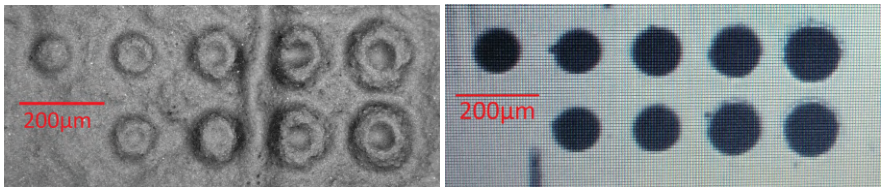

(a) (b)

Fig. 6.4: (a) Light microscope photo of marks in the donor of a Type 9 paste with a solder particle/flux mass ratio of $\approx$ 87/13 after a droplet transfer. The leftmost mark is just a hill. Further to the right the ditch around the hill becomes more clear. (b) Corresponding transferred droplets on the receiver. The image is from the screen of the laser work station.

Zero Mode

A zero-mode transfer means that no material is transferred to the receiver. This is caused if either the gap width is too large and the hill does not touch the receiver, or if the paste is to thick ($>$ 40 μm) or viscosity too high for the applied energy to bend the paste layer sufficiently. In the first case, the hills are still visible on the donor, while in the second case the hills can be very small or even indistinguishable from the normal unevenness of the paste layer and no marks are left at all.

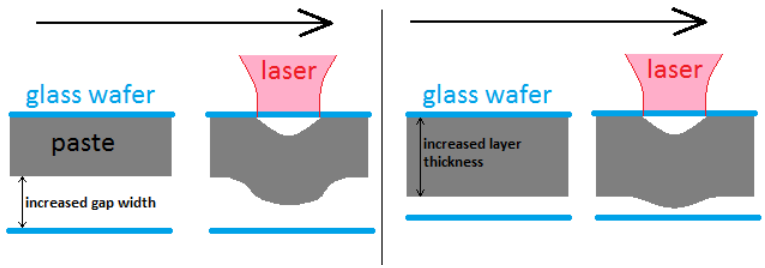

Fig. 6.5: Schematic of zero mode transfers.

Explosion Mode
Explosion transfers occur in two cases as well. Either the viscosity is very high or/and the paste layer is very thin (< 25 μm). For high viscosities the paste behaves as a solid and can not be bent. Instead a small amount of material breaks away from the layer and is pushed forward to the receiver during the LIFT process. The propelled material is not elastic enough to withstand the acting forces during the process and breaks into pieces. The resulting mark in the paste layer will be a hole (see figure 6.6a).

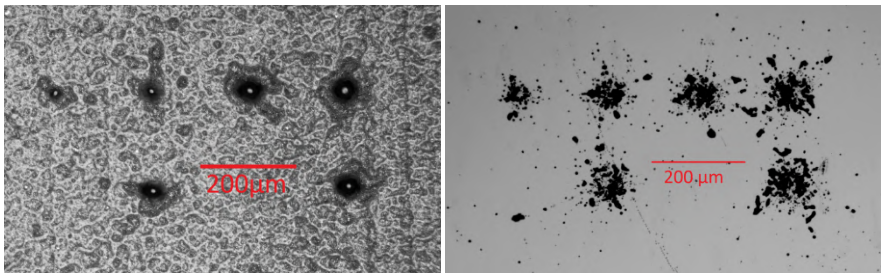

(a) (b)

Fig. 6.6: Explosion mode transfer. (a) Light microscope photo of holes in the donor of a Type 9 paste with a solder particle mass fraction larger than 87 % after an explosion transfer. The glass wafer, which carries the paste layer, is visible as the bright spot in the middle of the holes. (b) Corresponding transferred material on the receiver.

For thin layers with a sufficiently low viscosity the layer starts to bend, but as the gas volume increases the thin layer bursts and ”explodes”. The resulting mark in the paste layer is a small hole as well. The material surrounding the hole will slowly flow back into the hole due to the lower viscosity of the paste. Therefore the holes can be difficult to distinguish under the light microscope later.

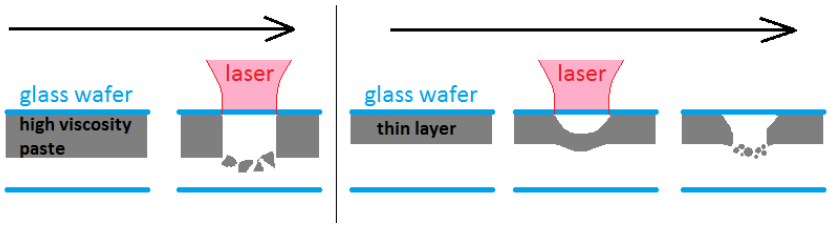

Fig. 6.7: Schematic of explosion mode transfers.

6.2.2 Influence of gap width, viscosity, layer thickness and laser power

Gap width

Of all four variables, the gap width is the main factor that limits droplet production. Droplets are only fabricated if the gap width is small enough for the hill in the paste layer to cross it and touch the receiver. If the gap is too wide, the hills cannot touch the receiver and no transfer will occur. A smaller gap can avoid the explosion of thin layers, because the hill will touch the receiver before it explodes and so the paste layer is held together. Furthermore, the material of an explosion distributes over a smaller area at small gap widths as shown in figure 6.8.

All pastes were tested with an average 5 μm and 0 μm gap width. Type 9 and type 6 solder pastes showed a higher probability of droplet production with 0 μm gap width. The production of droplets with less viscous nanopaste was successful also for a 5 μm gap width. It is assumed that larger drops are produced at low gap widths. Increasing the gap width will lead to smaller deposits, because the contact area between the hills on the donor and the receiver is decreased.

As explained in section 5.2, the spreading of the paste is not very precise. Furthermore the laser work station is not placed in a clean room and therefore small dust particles can be caught between the glass wafers causing differences in the gap width across the sample. Therefore the given gap widths can vary by several micrometers mak-

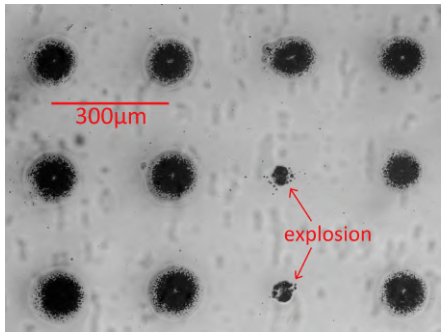

Fig. 6.8: Light microscope photo of droplets and two explosions of a Type 9 paste with a solder particle/flux mass ratio of $\approx$ 80/20. The large amount of droplets in this area indicates that the gap width is small ($<$ 5 μm). Compared to figure 6.6b, where the gap width was 25 $\pm$ 5 μm), the material of the two explosion transfers is distributed over a small area only.

ing it difficult to investigate the influence of the gap width further.

Viscosity

The effect of viscosity on the transfer mode and the drop size was studied in more detail. The nanopaste is 14 to 30 times less viscous than the solder pastes (see table 6.3). Successful trials with the nanopaste showed average drop diameters of one power between threshold and maximum available power in one trial between $\approx$ 300 μm and 1000 μm. While droplets of type 6 and type 9 solder paste are $\approx$ 40 to 260 μm in diameter on average over one power in one trial. Droplets produced with the less viscous nanopaste are always larger than droplets of solder paste, even if a larger gap width of 5 μm is used.

Different solder particle/flux mass ratios are mixed from type 9 solder powder and flux. The average droplet diameter over all produced droplets on one sample was calculated. The layer thicknesses of all samples were between 15 and 30 μm. Figure 6.9 indicates, that a decreasing solder mass fraction and a decreasing viscosity, respec-

tively, increase the average droplet diameter. The average increase of the droplet diameter is approximately 11 μm per solder fraction mass percent. This diagram includes only five trials. To reach more exact values and statistically proved results more successfully trials need to be performed.

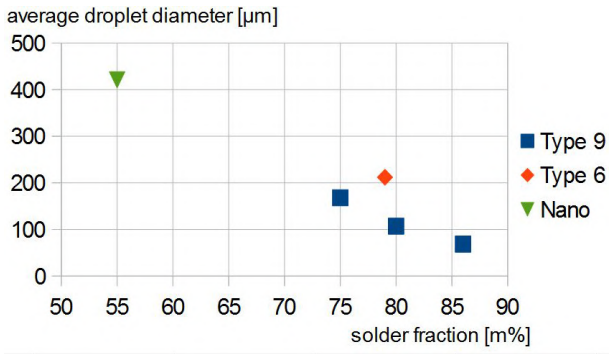

Fig. 6.9: The average drop diameter in μm over the solder mass fraction in mass percent. Although only five samples could be used for this analysis, the graphs show that increasing the solder fraction of the paste, decreases the average drop diameter.

A small variation in the solder fraction of only one percent changes the droplet size by ≈ 11 μm. It is known that due to the size variation of the solder spheres, the solder particles are not equally distributed over the whole sample. Therefore it is assumed that a variation of $\pm 1\%$ of the solder fraction occurs frequently in type 6 solder paste samples. In type 9 samples this variation should be smaller, because of the smaller size range of the solder particles. For the nanopaste this effect should be negligible for the droplet sizes that are reached with this process.

Type 9 pastes were mixed manually and insufficient mixing leads to variations in the paste viscosity. Therefore early trials with the same sample of type 9 paste showed very varying results. The differences in viscosity were even visible in the light microscope. Where

high viscosity samples appeared darker than samples with a lower viscosity. The high viscosity samples produced only explosion transfers and the marks in the donor were only holes (e.g. see fig. 6.10a and 6.6a). Therefore it is supposed that the probability of explosion transfers increases strongly for pastes with a solder particle mass fractions over 87%, which was the highest tested solder mass fraction.

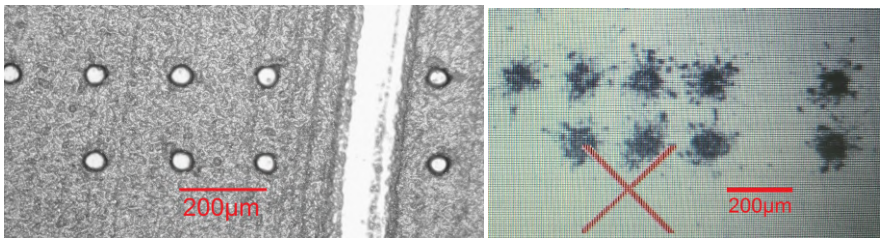

(a) (b)

Fig. 6.10: Explosion mode transfer. (a) Light microscope photo of holes in the donor of a type 9 paste with a solder particle mass fraction larger than 87 % after an explosion transfer. The glass wafer, which carries the paste layer, is visible as the bright circles. (b) Corresponding transferred material on the receiver imaged from the screen of the laser work station.

In experiments with nanopaste explosion mode transfers are not observed. It can be differentiated between a classical droplet transfer and a different kind of transfer where the hill in the paste layer does not touch the receiver. It is assumed that the low viscosity of the nanopaste lets the transferred material withstand the forces during the transfer. Therefore the transferred material stays together and does not ”explode” or break as it does for solder paste. Figure 6.11 shows the result of both transfer modes under the light microscope. The deposits in the top left and in the bottom right are produced by standard droplet transfer, while the other two are produced without the paste layer touching the receiver.

All successful experiments with nanopaste showed nearly 100% normal droplet transfers. Therefore, it is assumed that a low viscosity

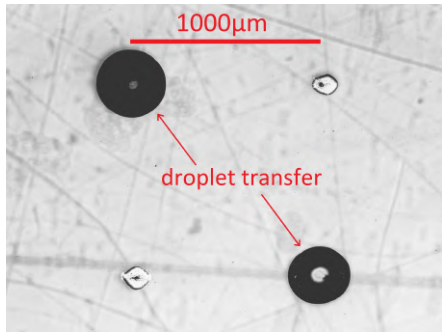

Fig. 6.11: Result of two different transfer modes imaged with a light microscope. The drop in the top left and in the bottom right are produced by normal droplet transfer, while the other two are produced without the paste layer touching the receiver.

increases the droplet fraction. Furthermore it was observed that the internal power threshold for nanopaste is approximately 0.5 W. For the solder pastes it is about 1.5 W. The low viscosity of the nanopaste lowers the threshold substantially. This effect is not observed for the smaller viscosity differences between different samples of the solder pastes. Other variables, especially the gap width, have a larger influence on the threshold power in that case.

Layer thickness

The experiments showed that an increasing layer thickness increased the drop diameter. The effect was most clear for trials with layers thicknesses 30 μm, 40 μm and 50 μm. Figures 9.2 and 9.3 in the appendix show the average droplet diameter over one power of one trial with nanopaste and one trial with type 6 solder paste. The gap width was 0 μm in both trials. As mentioned before, the nanopaste produces much larger drops than the solder paste, because of its low viscosity. For the nanopaste the average droplet diameter of a 40 μm thick layer is 234 μm to 345 μm larger than of a 30 μm layer. At the same thicknesses, the difference is only 11 μm to 31 μm for the type

6 paste.

Two samples of nanopaste were analysed regarding the average droplet diameter for every layer thickness over all trials of one sample. The results are summarized in figure 6.12. This graph shows clearly the correlation between layer thickness and droplet diameter. The slope of a linear approximation of the measured values, represents the mean increase rate of the droplet diameter s. It is 17.6 μm per micrometer thickness for the nanopaste with 55 % solder fraction.

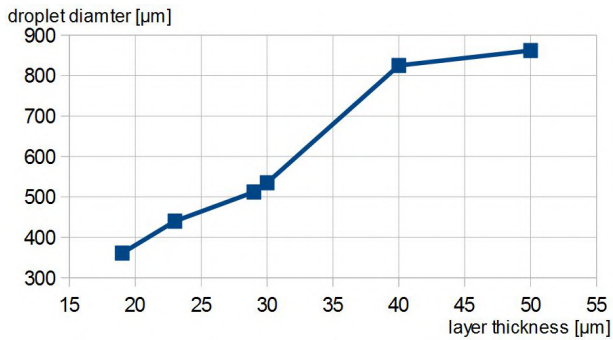

Fig. 6.12: Average droplet diameter over paste layer thickness for nanopaste with 55% solder fraction.

The measurement of type 9 solder pastes with three different solder fractions shows that the solder fraction influences s (see fig. 6.13). s is as low as 0,9 μm per micrometer thickness for the paste with 86 % solder mass fraction, but 6.2 μm per micrometer thickness for a solder fraction of 75 %. The mean diameter increase rate of the paste with 80 % solder fraction is 5.6 μm per micrometer thickness.

A type 6 paste with 87 % solder fraction was analysed as well. It has a mean increase rate of the droplet diameter s of 1.7 μm per micrometer thickness. The calculated values for s are summed up in figure 6.14. The points in figure 6.14 show clearly that the solder mass fraction and thereby the viscosity influences s. The mean diam-

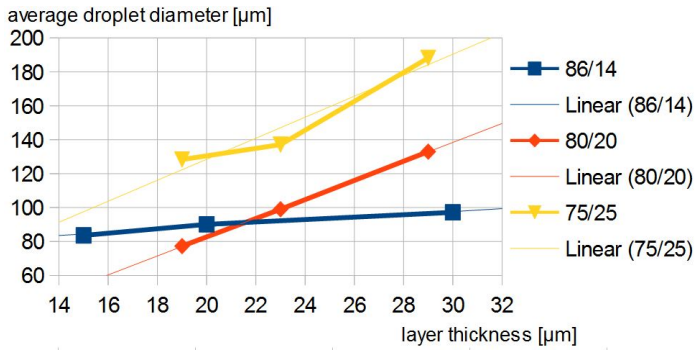

Fig. 6.13: Average droplet diameter over paste layer thickness for type 9 solder paste with (blue) 86 % (orange) 80 % and (yellow) 75 % solder fraction.

eter increase rate decreases 0.51 μm per micrometer thickness per percent solder mass fraction. Generally for a low viscosity the paste layer thickness will have a stronger influence on the droplet diameter.

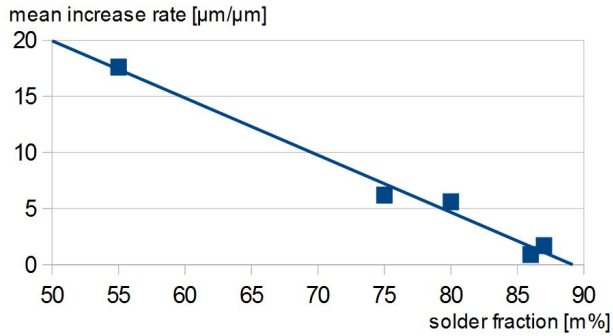

Fig. 6.14: Mean increase rate of the droplet diameter s over the solder mass fraction. The blue straight line is the trend line over all measurement points.

Figure 6.15 shows that for thicker layers ($>$ 23 μm) the probability of droplet transfers is higher than for thinner layers, because

thicker layers help to avoid explosion transfers. Again the results are influenced by the other variables, which leads to variations in the curves. For example the difference of the droplet fraction between the two type 6 (T6) samples at 29 and 30 μm layer thickness is caused by the higher viscosity of the sample represented by the green line. It is assumed that at higher viscosity more energy is needed to bend the paste layer and form a hill to overcome the gap width. Therefore the probability to produce a droplet decreases with increasing viscosity.

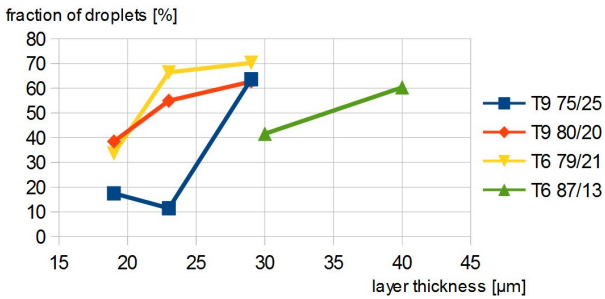

Fig. 6.15: Fraction of droplets over all possible pulses of several trials of four different samples over the layer thickness.

For layers thicker than 40 μm another effect influences the resulting transfer. A type 6 sample with 30 μm, 40 μm and 50 μm layers, produces droplets from the 30 μm and the 40 μm layer, but not from the 50 μm layer. The donor does not even show any marks in the 50 μm layer. Therefore it is assumed that if the layer is too thick, the layer does not bend enough to produce a hill that touches the receiver and no material is transferred. No hills are produced or they are so small that they are indistinguishable from the normal unevenness of the paste layer.

This effect can also explain the small difference of the droplet diameter between the 40 μm and the 50 μm layer of the nanopaste sample in figure 9.2. In this case, the 50 μm layer can still bend, because of the low viscosity of the nanopaste, but the bending is re-

strained by the layer thickness.

Laser power
The laser power does not influence the droplet diameter, but the number of droplets as shown in figure 6.16.

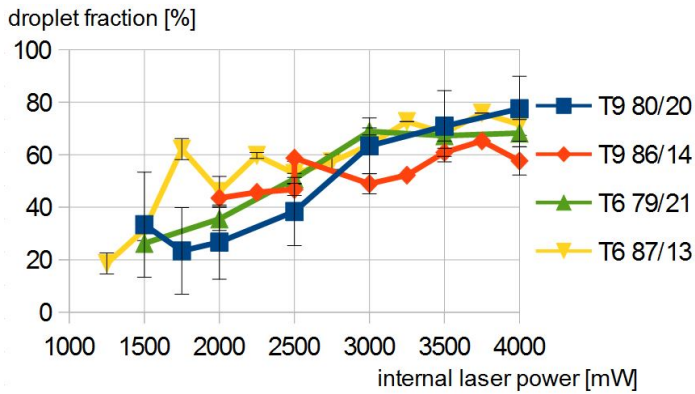

Fig. 6.16: Average droplet fraction over internal laser power for four different samples. The average was calculated over several successful trials per sample. (blue) and (orange) are of type 9 with 80 and 86 % solder mass fraction, respectively. (green) and (yellow) are of type 6 with 79 and 87 % solder mass fraction, respectively. Calculation of the shown error can be found in the appendix.

With increasing power the probability of droplet transfer increases. Between 1.5 W and 4 W internal laser power the droplet fraction increases from approximately 30 to 70 % for the type 6 pastes. The results vary more for the type 9 paste, but it is calculated that for this paste the droplet fraction between 2 W and 4 W internal laser power increases from approximately 35 % to 70 %. This analysis is done with a relatively small number of results for a statistically analysis more successful trials are necessary.

It is assumed that increasing the power produces a larger gas volume, which can lead to higher hills in the paste layer. Therefore an

increase of the laser power will increase the probability of the production of droplets.

When the power was above the threshold, the nanopaste showed nearly 100 % droplet fraction for all successful trials. It is concluded that a low viscosity increases the droplet fraction. This effect is barely visible in the curves in figure 6.16, which represents samples with small viscosity differences of just 7 % of the solder mass. The solder mass difference between the solder pastes and the nanopaste is 25 % to 32 %. Therefore the effect is stronger for the low viscous nanopaste.

At laser powers below the threshold no transfer will occur, because the force of the gas expansion initiated by a single laser pulse is too small to bend the paste layer or propel forward some material. The threshold power depends on the viscosity and the layer thickness of the paste and the gap width.

6.2.3 Summary of the influence of the parameters

The results show how careful the variables need to be adjusted to transfer single drops of solder paste. Especially choosing the right viscosity or solder/flux ratio is critical as the viscosity mainly determines how good the paste layer can be bent and it is an important solder paste property necessary for further work steps like attachment of surface mount components and reflow (see sec. 2.2.3 and 2.2.5). Generally a laser power high enough to create a gas expansion that can bend the paste layer and produce a hill is needed. The gap width determines if this hill touches the receiver or not. Viscosity and layer thickness should be chosen carefully to avoid explosion and zero-transfers.
Two variables influencing the resulting transfer, which are not investigated in detail in this thesis are the solder particle size and the laser spot size. Solder particles of different sizes are distributed in the paste layer. For a laser spot size in the range of the particle size the illuminated area can include just a single large solder sphere or several

small ones in extreme cases. This leads to variations in the amount of flux in the illuminated area and thereby the size of the gas volume. This would lead to unstable transfers and changing drop sizes. Increasing the laser spot diameter to three or four times of the particle diameter as in the performed experiments, decreases the probability of these variations and stabilizes the transfer and the drop size. The laser spot size could influence the drop size as well, because it affects the heat affected zone and thereby the area of gas evaporation.

6.3 Comparison to energy estimation

A method to estimate the energy required for a successful transfer was introduced in section 2.4. The internal laser threshold power for solder paste is approximately 1.5 W. Figure 6.16 shows that at $\approx$ 2.5 W ca. 50 % of the pulses produce droplets. Laser radiation power measurements estimate the power output at 2.5 W internal laser power to 1140 mW using a 2.5x objective (see figure 9.6 in appendix). The laser spot size is assumed to be similar to the spot in a 250 nm chromium layer. Using a 2.5x objective this spot is 35.5 μm in diameter at 2.5 W internal power. The internal power is given as the average power. The energy per pulse is calculated according to the formula in section 2.3.

$$E_{pulse} = \frac{1140\,\text{mW}}{100\,\text{kHz}} = 11.4\,\mu\text{J}$$

Furthermore the bending of the layer induced by solvent evaporation needs to cross the gap width. Successful experiments with solder paste showed that the gap width needs to be smaller than 5 μm, probably closer to 1 μm. Likely, the gas volume would need to reach a height of at least 2.5 μm to guarantee proper attachment of the paste to the receiver.

To estimate the gas volume, some information about the thermal constants of the solvents is needed. Table 6.4 shows the values of two typical solvents.

Table 6.4: Thermal constants of Ethanol and Diethylene Glycol Monobutyl Ether [52, 53]

Solvent	Ethanol	DGM ether
Boiling temperature in K	353	504
c_p in $\frac{\mathrm{J}}{\mathrm{kg \cdot K}}$	$2.57 \cdot 10^3$	$2.219 \cdot 10^3$
c_v in $\frac{\mathrm{J}}{\mathrm{kg}}$	$9.11 \cdot 10^5$	$3.10 \cdot 10^5$

Using all these values and calculating E_s using equation 4 gives $E_s =$ 3.97 nJ for ethanol and 2.03 nJ for DGM ether. From these values the input energy E_{in} can be calculated from equations 1 and 3. This energy should equal E_{pulse}. The calculated input energies are 25.3 nJ and 12.9 nJ for ethanol and DGM ether, respectively. This is orders of magnitudes smaller than E_{pulse}, which means that the estimation is insufficient.

It is supposed that the most unrealistic part of the estimation is to assume that the sticky force F_{sticky} is neglectable. Therefore another approach was used to estimate the influence of the stickiness of the paste.

In the estimation introduced in section 2.4 it was assumed that a voxel needs to detach completely from the layer to produce a droplet. The results show that this is not true. Instead the paste layer needs to be bent, inducing shear stress in the paste. The properties of the paste apply a force against this bending, which explains the increased energy needs.

To simplify the calculations, it is assumed that the behaviour of the paste is Newtonian. From section 2.1 we know that the shear stress of Newtonian fluids is calculated as:

$$\tau = \mu \frac{dv}{dy}$$

Furthermore, in a first approach the shear stress is defined as:

$$\tau = \frac{F}{A}$$

with the applied force F and the cross-sectional area A parallel to F. In the case of bending the paste layer, this force is applied by the gas volume and can be calculated as:

$$F_{bend} = \mu \frac{dv}{dy} \cdot A$$

The force of the gas volume pushes the paste forward and induces a certain shear rate in the paste layer. For simplicity, it is assumed that the force of the increasing gas volume is applied in a circle in the centre of the laser spot as shown in figure 9.8 in the appendix.

Furthermore, it is assumed that the shear rate $\frac{dv}{dy}$ is constant over the whole moved area leading to:

$$\frac{dv}{dy} = \frac{2v_0}{r}$$

The area parallel to the applied force can be approximated by the side of a cylinder with a diameter equal to the radius of the laser spot r and a height equal to the layer thickness x. This gives:

$$A = \pi \cdot r \cdot x$$

Putting all this in the formula for F_{bend} gives:

$$F_{bend} = \mu \frac{v_0}{r} \cdot \pi \cdot r \cdot x$$

Finally F_{bend} needs to be included in $F_{gas} \geq F_{sticky} + F_o$. This can be ransformed into a formula for E_s and gives:

$$E_s = (F_{bend} + \pi r^2 \cdot p_0) \cdot \frac{h}{R_s \cdot T} \cdot (c_p \cdot \Delta T + c_V)$$

Different values of viscosity μ , gas volume height h and velocity v_0 can be assumed to give the $E_{in} = E_{pulse}$. An overview is given in table 6.5. Table 6.5 includes reasonable values of the variables and shows that taking the force necessary to bend the paste layer into account results in $E_{in} = E_{pulse}$.

Table 6.5: Values of gas volume height, viscosity and velocity to give $E_{in} = 11,4\ \mu$m. Ethanol is assumed as the used solvent.

Gas volume height h in μm	2.5	5	7.5	5	5	5
Viscosity μ in Pa·s	250	250	250	300	200	100
Velocity v_0 in $\frac{\text{m}}{\text{s}}$	0.96	0.48	0.32	0.40	0.60	1.2
F_{bend} in mN	45.2	22.6	15.0	22.6	22.6	22.6
E_{in} in μJ	11.4	11.4	11.4	11.4	11.4	11.4

7 Discussion

7.1 LIFT of single solder balls

As mentioned in section 5.1 and 6.1, it is assumed that the particle size distribution and the variation of the amount of flux around the solder spheres causes variations of the measured threshold energies. These assumptions could be easily proved with a paste including particles of only one size. Unfortunately, such a paste is not commercially available today. Furthermore the goal of this part of the thesis was to show, that small, single particles can be transferred by a fs laser pulse. This was successfully done and therefore it was decided to not continue with this kind of experiment.

Therefore the results offer an indicator for the right order of magnitude for the threshold energy, but are not exact values. Furthermore the influence of the spreading method could be studied more detailed to understand how it influences the flux distribution around

the particles and thereby the threshold energy. This might be difficult, because the flux is transparent. But with the right dye and an appropriate microscope it should be possible.

7.2 LIFT of solder paste droplets

Figure 7.1 indicates the difficulties with this kind of experiments. The applied parameters should be the same along one row and therefore the same transfer mode is expected for all pulses in one row. In reality this is not the case. Instead one pulse can transfer a clean droplet and the next one can cause an explosion transfer. In the part of an experiment, shown in figure 7.1, 50 % of the transfers are droplets and 50 % are explosions. This shows that the main difficulty of these experiments is to keep constant conditions on one sample.

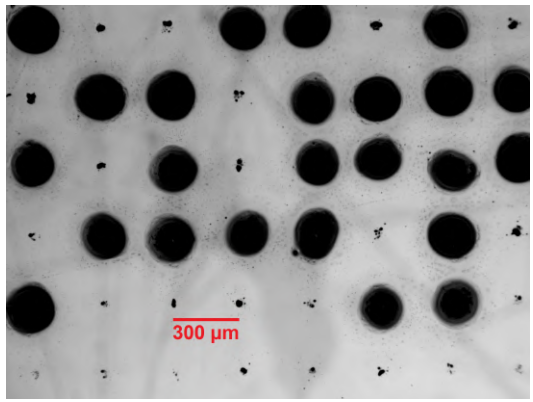

Fig. 7.1: Transferred material of a 23 μm layer of type 6 solder paste with a solder mass fraction of 79 %. The internal laser power is increasing from 2 W in the bottom to 4 W in the top. The power is constant in every row.

As explained in section 6.2.2, it is assumed that mainly the four variables gap width, viscosity, layer thickness and laser power influence the transfer. The laser power could be set to a distinct value

for every pulse. The other three parameters varied due to the used sample preparation method.

The gap width can vary by some micrometers due to dust particles between the glass slides. The layer thickness changes by some micrometers too, because of the spreading method. A change in the layer thickness leads also to a change of the gap width. The viscosity is not constant over the whole sample, as well. The solder particle/flux mass ratio changes due to the size distribution of the solder particles. This effect decreases for layers over 30 μm. For pastes, which are mixed manually, the variation in viscosity can be prevented by thorough mixing. Commercial pastes, which have been quality checked at the factory, are a more reliable alternative.

To achieve more constant transfers, it is important to find a way to spread the paste with a uniform layer thickness. This would also decrease the gap width variation. The experiments and data analyses indicate that the gap width is the most critical variable. Small changes of a few micrometers can change the transfer mode and it is difficult to set the gap width precisely for distances below 5 μm.

Generally, for one single pulse it is unknown which variable caused a changed transfer mode or influenced the droplet diameter. In a successful experiment 500 to 1000 droplets could be produced from one sample. Analysing a successful experiment leads to statistically reliable results, which provide insights about the processes and the affecting variables.

The success of the experiment can only be determined after removing the donor from the receiver. It is not possible to observe any effects of the gas bubble on the backside of the paste layer, because the solder particles scatter the imaging light too much. One sample might be radiated by a thousand pulses, but none of these transferred a single droplet. The result is unknown until the donor is removed from the receiver. For the nanopaste, where the light is scattered less, the effect of the gas bubble is visible and a droplet and an explosion transfer are clearly distinguishable (see fig. 9.9 in the appendix).

In section 6.2.1 three transfer modes of solder paste were identified. These transfer modes are in line with findings by Munoz-Martin et. al. (2016) who investigated ”Laser-induced forward transfer of high-viscosity silver pastes”. The scientists used a silver paste with a particle size of 1 μm to 4 μm and a viscosity of $\approx$ 250 Pa·s by single Gaussian nanosecond laser pulses [9]. The particle size is similar to type 9 solder paste and the viscosity is similar to type 6 and type 9 pastes. In this article four transfer mechanisms were identified. Figure 7.2 shows a schematic of these four transfer mechanisms.

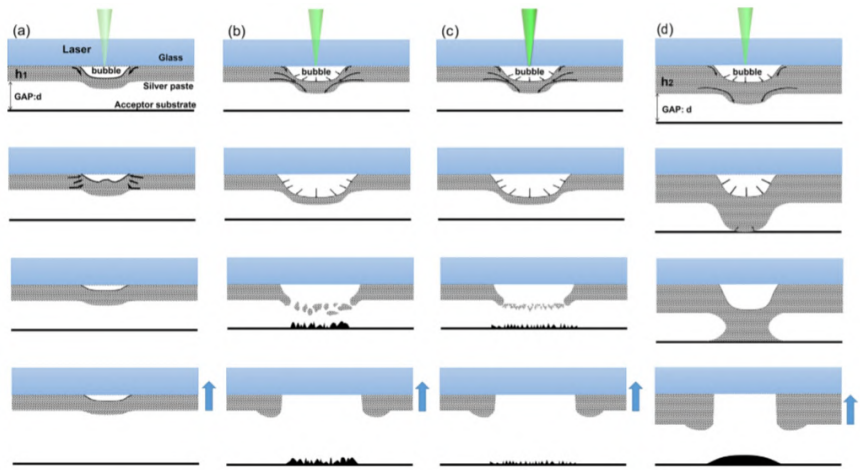

Fig. 7.2: Schematic of transfer mechanisms for varying laser peak fluences and donor thicknesses with a fixed gap distance: (a) blister formation, when the fluence is below the threshold; (b) cluster-dot transfer, for fluences slightly above the threshold; (c) explosion-dot transfer, when the fluence is much higher than the threshold; and (d) concrete-dot transfer, when the donor is thick enough relative to the gap that the acceptor prevents fragmentation during transfer. The bottom image in each column shows the final voxel obtained after removing the donor. [9]

The scientists conclude that in ”concrete-dot transfer”, which is identical to the droplet mode, ”the donor thickness h is large enough

relative to the gap d" that the paste hill reaches the receiver while it is still connected to the donor substrate. When the hill reaches the receiver, "confinements prevent the paste from fragmenting into pieces." The used paste layer thickness was 50 μm to 60 μm and the gap width was 50 μm or 140 μm. They showed that thinner paste layers (30 - 35 μm) at the same gap width produce "cluster-dot transfer" and "explosion-dot transfer", which correspond to the explosion mode in this thesis. The described "blister formation" is similar to the zero mode of this thesis. The huge difference between the experiments in this thesis is the used gap width. It seems the properties of the solder paste confine the gap width to a much smaller range of some micrometers for droplet transfers, while for silver paste, the gap width can be at least 140 μm, if the paste layer is thick enough.

As mentioned in section 2.5 Mathew et.al. (2015) successfully transferred type 7 solder paste. To prove if the results of this thesis are in a reasonable range the settings and the results of the article and this thesis are compared in table 7.1.

Table 7.1: Settings of the experiments with solder paste from the article [5] and this thesis. *The laser spot diameter is estimated from figure 9.7 in the appendix.

	Article	Thesis
Laser beam shape	tophat	nearly gaussian
Gap width in μm	0 or 25	0-5
Layer thickness in μm	10-25	15-50
Best results for	18-20	25-40
Laser spot diameter in μm	33, 45, 80, 115	15-38*

In the experiments in the article clean deposits could be transferred for all combinations of gap widths and laser spots except for a 25 μm gap width and a 33 μm laser spot. For these settings the transferred material showed "some degree of "splatter" with flux

and occasionally solder beads landing in regions between desired locations."[5]. In this thesis the laser spots are smaller and it is more difficult to reach a stable production of droplets. Munoz-Martin et. al., who used a laser spot of only 12.5 μm observed explosion mode transfers as well [9]. It is concluded that one reason for the difficulties in the droplet production is the small diameter of the laser spot. Hence it is assumed that for the same reason larger laser powers, which lead to a larger laser spot, produce more droplets than smaller powers (see Laser Power in sec. 6.2.2).

For a 0 μm gap the diameter of the transferred droplets described by Mathew et.al. [5] are only 10 μm to 15 μm larger than the laser spot diameter. In this thesis droplets are between 40 μm and 260 μm depending on the paste properties and laser power. This is nearly seven times larger than the laser spot. In the article by Munoz-Martin et. al. a laser spot of 12.5 μm and a Gaussian beam was used and they reached droplet diameters between 100 μm and 250 μm depending on the laser power. This is up to 20 times larger than the laser spot. It is supposed that the energy distribution of the laser beam is a very important factor for the resulting droplet diameter. In a top hat beam the energy is constant over nearly the whole laser spot. Therefore solvent evaporation could occur uniformly over the illuminated area and material is mainly pushed forward. A Gaussian beam has an energy peak at the centre and radiation energy decreases towards the edge of the illuminated area. As shown in figure 7.3, the amount of evaporated solvent will be larger in the centre than in the outer areas and material will be pushed forward and sideways. Depending on the particle distribution, more or less paste could be pushed to the side or forward, which also affects the droplet production.

The article gives threshold fluences F to transfer type 7 solder paste. The threshold energy E is defined as:

$$E = F \cdot A = F \cdot \pi r^2$$

with the laser spot area A and the laser spot radius r. The calculated

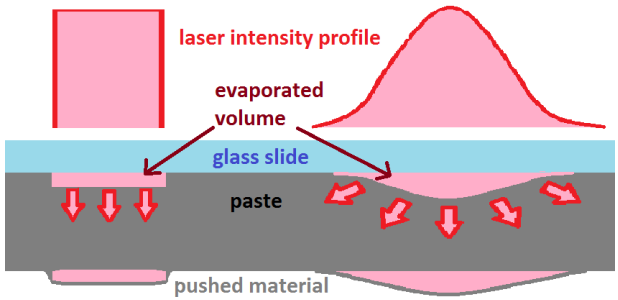

Fig. 7.3: Schematic of the solvent evaporation and the movement of material during LIFT with (left) a tophat laser beam and (right) a Gaussian beam

threshold pulse energies are 2.35 μJ for a 33 μm laser spot diameter to 11.31 μJ for a 80 μm laser spot diameter. As calculated in section 6.3, the pulse energy to produce droplets for 50% of all pulses is 11.4 μJ. Droplets are already produced at 6.7 μJ, which corresponds to 1.5 W internal power. Both values are in the same order of magnitude as the threshold energies presented in the article. Comparing the threshold energies and the laser spot sizes, the energies from the article are smaller. One reason for this could be the different laser beam shape. In the article a top-hat beam was used, while a Gaussian beam was used in this thesis. To reach the same area were the laser energy is larger than the threshold, the Gaussian beam needs a larger total pulse energy.

Finally, it can be concluded that further experiments should be performed with a tophat beam to reach smaller deposits and a stable droplet production. Larger laser spots might also lead to a more stable droplet production. Then conditions for a stable droplet production could be found without a need for small gap widths below 5 μm. This would increase the possibility for industrial use of LIFT of solder paste.

8 Summary

The microelectronics industry aims to bring ever smaller devices to the market. A major challenge, especially in the production of medical devices, is the development of diminutive sensors and device components [10], and the precise fitting of surface mounted components on circuit boards. One technology to overcome the prevailing problems and limits is Laser-Induced Forward Transfer (LIFT).

LIFT is a technology used to print different kinds of materials directly on to a receiver with a higher resolution than common printing technologies. Different companies use the technique already to catapult cells and parts of tissue away from surrounding tissue [56], to print ceramic inks on car glass and ceramics [57] or to print biomaterials for high resolution tissue engineering [58].

The method is very precise and can be used to apply solder paste as well. Solder paste is used to form solder joints between the circuit board and surface mounted components. The smallest solder paste droplets produced today are $\approx$ 200 μm in diameter. Producing smaller droplets will save material and space. Hence electrical devices and sensors can be fabricated even smaller.

In this thesis single solder particles were successfully transferred from type 5 solder paste using different objective magnifications and laser wavelengths. It is shown that the transfer of very small particles ($\approx$ 10 μm) is possible and that the resolution of this method is mainly limited by the size of the transferred particle, not by the method itself.

The measurements indicate that the necessary energy to transfer a particle increases with the size of the particle. The necessary energy increases approximately with 6,2 nJ per micrometer diameter. Depending on the amount of flux above or underneath the particle the necessary energy to transfer a particle might differ. It is supposed that the way of paste spreading influences the distribution of flux around the solder particles.

Successful transfer of clean droplets between 40 μm and 260 μm

could be shown for a type 6 and a type 9 solder paste as well. The transfer is mainly influenced by four variables: the gap width, the paste viscosity, the layer thickness and the laser power. Different combinations of these variables lead to three transfer modes, which are called ”droplet”, ”zero” and ”explosion”. The variables cause also the size variation of the droplet.

The droplet mode is the only transfer to produce clean deposits. In this mode the laser radiation deposits the right amount of energy in the flux to evaporate enough solvents and bend the paste layer. The bent layer touches the receiver and when the donor is removed, the droplet is formed on the receiver.

From the performed experiments and their analyses it is supposed that the gap width is the most critical variable. Only a small change of some micrometers can change the transfer mode and it is very difficult to set the right gap width, which is below 5 μm. Also the other variables need to be adjusted very carefully to reach the droplet mode and to suit further work steps. Especially to choose the right viscosity or solder/flux ratio can be demanding as the viscosity determines how good the paste layer can be bent and it is an important solder paste property for further work steps.

Generally a laser power great enough to bend the paste layer and produce a hill is needed. The gap width determines if this hill touches the receiver or not. To avoid explosion and zero-transfers, viscosity and layer thickness should be chosen carefully.

Based on this work it is assumed that smaller metal particles should be used to reach a better resolution for LIFT of solder paste. On the other hand, smaller particles do increase the metal surface and thereby the oxide content, which leads to solder joints of lower quality. Adding flux base and activators avoids oxidation, but it would change the rheological properties of the paste. A higher flux fraction decreases the viscosity, which will lead to undesired higher slump and lower tackiness and finally to a lower quality of the solder joint as well.

9 Outlook

In summary, the properties of the paste need to be well balanced for the different requirements. Therefore it is difficult to define the best combination of materials for a solder paste used in a LIFT process. Currently there is no special LIFT-solder paste commercially available.

Finally, it can be concluded that further experiments should be performed with a tophat beam to reach smaller deposits and a stable droplet production. Larger laser spots might also lead to a more stable production. Under these conditions the droplet mode might be possible without the need for extremely small gaps smaller than 5 μm. This would increase the possibility of industrial use of LIFT of solder paste.

References

[1] R.S. Braudy,
Laser Writing
Proc. IEEE 1969, 57, 1771. (1969).

[2] M. L. Levene, R. D. Scott, and B. W. Siryj,
Material Transfer Recording
Appl. Opt. 9, 2260-2265 (1970).

[3] J. Bohandy, B. F. Kim, F. J. Adrian,
Metal deposition from a supported film using an excimer laser
J. Appl. Phys., 60, 1538 (1986)

[4] Pere Serra and Alberto Piqué,
Laser-Induced Forward Transfer: Fundamentals and Applications
Adv. Mater. Technol., 4, 1800099 (2019)

[5] S. A. Mathews, N. A. Charipar, R. C.Y. Auyeung, H. Kim, A. Piqué,
Laser forward transfer of solder paste for microelectronics fabrication
Proc. SPIE 9351, Laser-based Micro- and Nanoprocessing IX, 93510Y (2015)

[6] S. A. Mathews, R. C. Y. Auyeung, H. Kim, N. A. Charipar, and A. Piqué,
High-speed video study of laser-induced forward transfer of silver nano-suspensions
J. Appl. Phys. 114, 064910 (2013)

[7] J. Wang, R. C. Y. Auyeung, H. Kim, N. A. Charipar, A. Piqué,
Three-Dimensional Printing of Interconnects by Laser Direct-Write of Silver Nanopastes
Adv. Mater. 22, 4462.(2010).

[8] H. Kim, M. Duocastella, N. A. Charipar, R. C. Y. Auyeung, A. Piqué,

Laser printing of conformal and multi-level 3D interconnects
Applied Physics A, Vol.113(1), pp.5-8 (2013)

[9] D.Munoz-Martin, C.F. Brasz, Y.Chen, , M.Moralesa, C.B. Arnold, C. Molpeceresa,
Laser-induced forward transfer of high-viscosity silver pastes
Applied Surface Science. 366. 389-396 (2016)

[10] J. R. H. Shaw-Stewart, T. Mattle, T. K. Lippert, M. Nagel, F. A. Nueesch, A. Wokaun,
The fabrication of small organic light-emitting diode pixels by laser-induced forward transfer
Journal of Applied Physics 113, 043104 (2013)

[11] D. P. Bank, K. S. Kaur, C. Grivas, C. Sones, P. Gangopadhyay, C. Ying, J. D. Mills, S. Mailis, I. Zergioti, R. Fardel, M. Nagel, T. Lippert, X. Xu, S. P. Banks, R. W. Eason,
Femtosecond laser-induced forward transfer for the deposition of nanoscale, transparent, and solid-phase material
Proceedings of LAMP (2009)

[12] S. Bera, A. J. Sabbah, J. M. Yarbrough, C. G. Allen, B. Winters, C. G. Durfee, J. A. Squier,
Optimization Study of the Femtosecond Laser-induced Forward-transfer Process with thin Aluminium Films
APPLIED OPTICS Vol. 46, No. 21 (2007)

[13] M. Sanz, M. Walczak, M.Oujja, C. Domingo, A. Klini, E.L. Papadopoulou, C. Fotakis, M. Castillejo,
Femtosecond laser deposition of TiO_2 by laser induced forward transfer
Thin Film Solids 518 5525-5529 (2010)

[14] C. Germain, Y. Y. Tsui,
Femtosecond Laser Induced forward Transfer of Materials
Proceedings of ICMENS (2003)

[15] F. A. Morrison,
Understanding Rheology
New York: Oxford University Press (2001)

[16] N. Phan-Thien, N. Mai-Duy,
Understanding Viscoelasticity
3rd Edition, 2017

[17] Electronics Notes: What is Solder Paste& How to Use it
`https://www.electronics-notes.com/articles/constructional_techniques/soldering/solder-paste-how-to-use.php`
03/12/2019

[18] Global Solder Solutions: Solder Paste Powder: When to Downsize
`https://aimsolder.com/technical-articles/solder-paste-powder-when-downsize`
03/12/2019

[19] R. Lapasin, V. Sirtori, D. Casati,
Rheological Characterization of Solder Pastes
Journal of Electronic Materials, Vol. 23, No. 6 (1994)

[20] Y. Wang, X. Xu, J. Zhou, F. Xue, *Investigation of Rheology Behavior of Lead-free Solder Paste*
16th International Conference on Electronic Packaging Technology (2015)

[21] F.V. Barbosa et al.
Rheological Characterization of Solder Paste
Proceedings of the ASME 2017 International Mechanical Engineering Congress and Exposition (2017)

[22] A,Pietrikova, M. Kravcik,
Investigation of Rheology Behavior of Solder Paste
35th Int. Spring Seminar on Electronics Technology (2012)

[23] J.W. Evans, H.K. Beddow,
Characterization of Particle Morphology and Rheological Behavior in Solder Paste
IEEE Transactions on Componente, Hybrids and Manufacturing Technology. Vol. CHMT-10, No. 2 (1987)

[24] Chegg Study: Simple Shear Flow Between Parallel Plates
https://www.chegg.com/homework-help/questions-and-answers/simple-shear-flow-parallel-plates-consider-flow-incompressible-newtonian-fluid-parallel-pl-q14690247
16/12/2019

[25] H. A. Barnes,
Thixotropy - a review
Journal of Non-Newtonian Fluid Mech., 70, 1-33 (1997)

[26] Polymer Innovation Blog: Polymers in Electronic Packaging: What is the Thixotropic Index? 2018 By Jeffrey Gotro
https://polymerinnovationblog.com/polymers-in-electronic-packaging-what-is-the-thixotropic-index/
04/02/2020

[27] Polymer Properties Database: ROSIN ESTERS AND POLYMERS
https://polymerdatabase.com/polymer%20classes/Rosin.html
17/01/2020

[28] Google Patents: Flux for lead-free solder, and lead-free solder paste
https://patents.google.com/patent/WO2016199747A1/en
17/01/2020

[29] KOKI Company Limited: General Information on Solder Paste
http://www.pmdtkt.upc.smm.lt/dokumentai/Medziaga

/inzinerine/mm12/Priedai/3_4%20priedas.%2023
_Solder_paste_general_info_KOKI.pdf
22/01/2020

[30] Bilek, J., et al.,
Thermal Conductivity of Molten Lead Free Solders
European Microelectronics and Packaging Symposium, Czech Republic. (2004)

[31] The Engineering ToolBox: Thermal Conductivities for some common Liquids
https://www.engineeringtoolbox.com/thermal-conductivity-liquids-d_1260.html
27/01/2020

[32] Senju Metal Industry Co., Ltd.: M705-LFAC19
https://www.tempoautomation.com/wp-content/uploads/2018/04/M705Senju_Lead_Free.pdf
30/01/2020

[33] alpha: ALPHA JP-500 Solder Paste
https://alphaassembly.com/Products/Solder-Paste/JP-500
28/04/2020

[34] alpha: ALPHA JP-500 Product Guide
https://www.google.de/url?sa=t&rct=j&q=&esrc=s&source=web&cd=2&ved=2ahUKEwjm_tXKlIvpAhVhpIsKHbhVDB8QFjABegQIBxAB&url=https%3A%2F%2Falphaassembly.com%2F-%2Fmedia%2FFiles%2FCookson Electronics%2FProducts%2FSolder-Paste%2FProduct-Guide%2F20111206--ALPHA-JP500--Product-Guide.pdf&usg=AOvVaw2whnYdkQLdnKqIjE9zgoyn
28/04/2020

[35] 5N Plus Micro Powders
https://www.5nplus.com/micro-powders.html
28/04/2020

[36] Sigma-Aldrich: Silver nanoparticles ink for screen printing
https://www.sigmaaldrich.com/catalog/product/aldrich/901090?lang=en&region=SE
28/04/2020

[37] ECO Solder Paste: M705-ULT369 Technical Report
https://www.eurocircuits.com/wp-content/uploads/TC-1711017AG-M705-ULT369-Technical-Report-1.0E.pdf
30/01/2020

[38] N.-C. Lee,
Reflow Soldering Processes and Troubleshooting: SMT, BGA, CSP, and Flip Chip Technologies
Newnes/Butterworth-Heinemann p.4/77-4/84 (2002)

[39] J. Bath (Editor)
Lead-Free Soldering
Springer p.78-81 (2007)

[40] Tamura Product Information: Pb-Free Solder Paste TLF-Series LF Solder TLF-4011
http://www.hapoin.com/upload/20170407150708fujian_groupcopy4.pdf
04/02/2020

[41] Farnell: Product Data Sheet, MP200, October 2002
http://www.farnell.com/datasheets/1738696.pdf
04/02/2020

[42] Fei He et. al.,
Femtosecond Laser Fabrication of Monolithically Integrated Mi-

crofluidic Sensors in Glass
Sensors 14 (2014)

[43] T. Mans, J. Dolkemeyer, C. Schnitzler,
High Power Femtosecond Lasers: Efficient power scaling of ultrashort-pulse lasers to kW range and more
Laser Technik Journal 3 (2014)

[44] IMRA: What Does Cold Ablation Really Mean?
https://www.imra.com/what-does-cold-ablation-really-mean/
11/02/2020

[45] K. Sugioka, Y Cheng,
Femtosecond laser three-dimensional micro- and nanofabrication
Applied Physics Reviews 1 (2014)

[46] Characteristics of Solder Paste
http://www.idc-online.com/technical_references/pdfs/mechanical_engineering/Characteristics_of%20Solder_Paste.pdf
11/02/2020

[47] Harima: Sn-3.0Ag-0.5Cu lead-free solder paste
https://www.harima.co.jp/products/electronics/pdf/brochure18e_18.pdf
12/02/2020

[48] C. Billotte, P. J. Carreau, M.-C. Heuzey,
Rheological characterization of a solder paste for surface mount applications
Rheol Acta 45: 374-386 (2006)

[49] H. A. Barnes,
The yield stress-a review or- 'παντα ρει' - everything flows?
Journal of Non-Newtonian Fluid Mechanics Volume 81, Issues 1-2, Pages 133-178 (1999)

[50] Z. Cheng, X. XiaoYan, Z. Jian, X. Feng,
The effect of flux components on the slump-in-heating resistance of Sn-3.0Ag-O.5Cu solder paste
16th International Conference on Electronic Packaging Technology (2015)

[51] PVlighthouse: METAL REFLECTANCE BEFORE AND AFTER ENCAPSULATION
https://www.pvlighthouse.com.au/cms/lectures/white-papers/optical/mr-metal-reflectance
17/02/2020

[52] The Engineering Toolbox: Ethanol - Thermophysical properties
https://www.engineeringtoolbox.com/ethanol-ethyl-alcohol-properties-C2H6O-d_2027.html
06/03/2020

[53] Diethylene Glycol Monobutyl Ether
https://m.cameochemicals.noaa.gov/chris/DME.pdf
28/04/2020

[54] Y.K. Wu, K.L. Lin, B. Salam,
Specific Heat Capacities of Sn-Zn-Based Solders and Sn-Ag-Cu Solders Measured Using Differential Scanning Calorimetry
Journal of ELECTRONIC MATERIALS, Vol. 38, No. 2, 2009

[55] The Engineering Toolbox: Specific Heat of Solids
https://www.engineeringtoolbox.com/specific-heat-solids-d_154.html
06/03/2020

[56] Zeiss: Laser Microdissection with ZEISS PALM MicroBeam
https://www.zeiss.com/microscopy/int/products/laser-microdissection/microbeam.html
29/04/2020

[57] LPKF: Digitaler Druck von keramischen Farben
https://www.lpkf.com/de/branchen-technologien/ueber-digitalen-laser-transferdruck/
29/04/2020

[58] Poietis: 4D Laser-assisted Bioprinting
https://poietis.com/4d-laser-assisted-bioprinting/
29/04/2020

Appendix

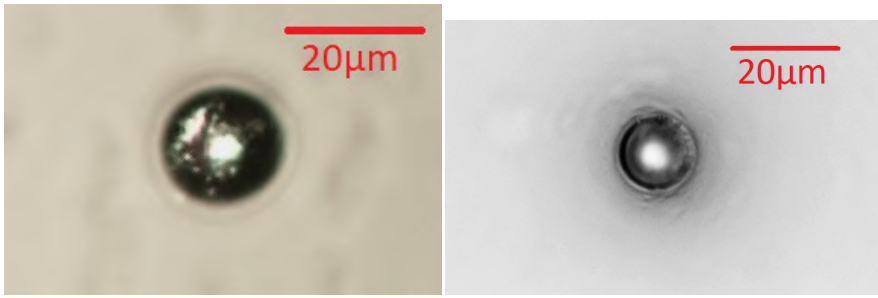

Fig. 9.1: Transferred single balls of type 5 solder paste imaged with a light microscope. The metallic shiny spot in the centre of the particles is typical for solder spheres watched at high magnification.

Calculation of the error in figure 9.2, 9.3 and 6.16
The error e is defined as:

$$e = \frac{s_d}{\sqrt{N}}$$

where N is the number of values and s_d is the standard deviation defined as:

$$s_d = \sqrt{\frac{\sum_{i=1}^{N} (x_i - \overline{x})^2}{N}}$$

with the average over all values $\overline{x}$.

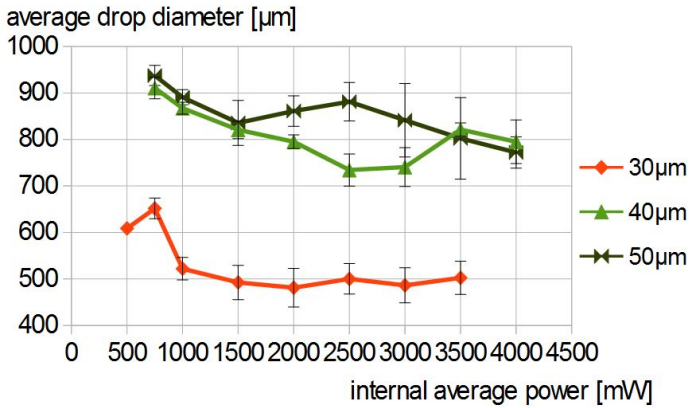

Fig. 9.2: Average droplet diameter over internal power of the laser for different layer thicknesses of nanopaste. Calculation of the shown error can be found in the appendix.

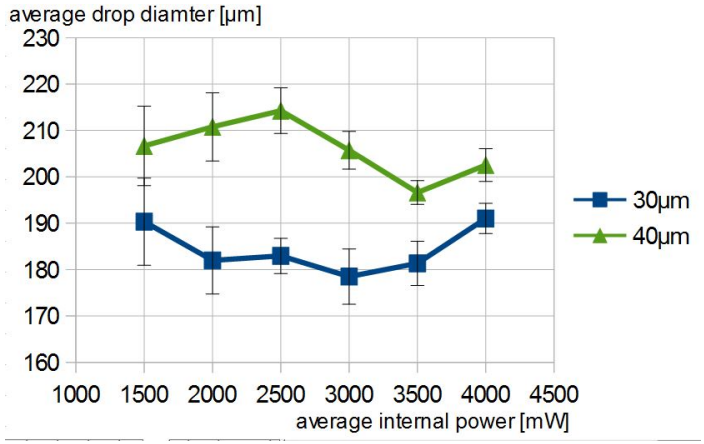

Fig. 9.3: Average droplet diameter over internal power of the laser for different layer thicknesses of a trial of type 6 paste with solder particle/mass ratio = 87/13. Calculation of the shown error can be found in the appendix.

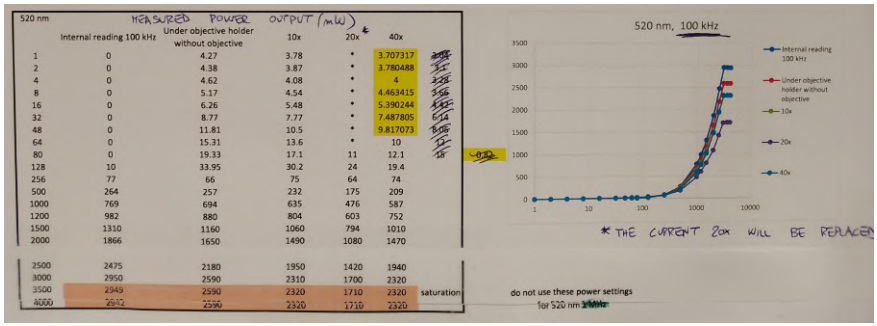

Fig. 9.4: Output power of the laser radiation with a wavelength of 520 nm and a frequency of 100 kHz at different places in the laser workstation and using different objectives. Measured and provided by the tool responsible.

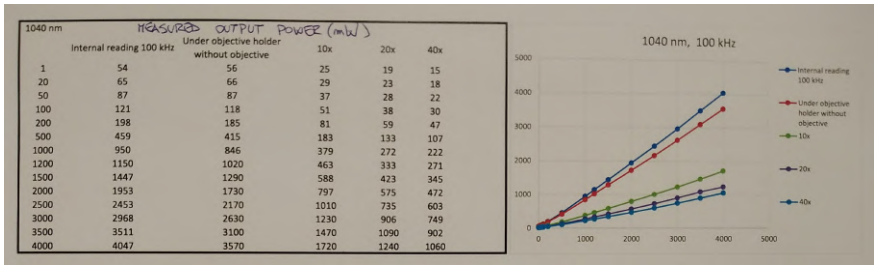

Fig. 9.5: Output power of the laser radiation with a wavelength of 1040 nm and a frequency of 100 kHz at different places in the laser workstation and using different objectives. Measured and provided by the tool responsible.

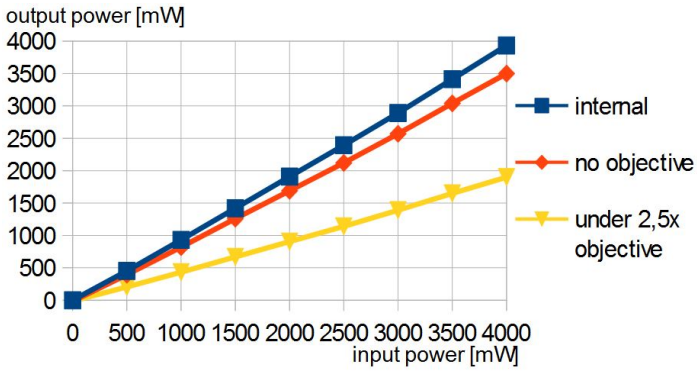

Fig. 9.6: Measured average laser powers at different positions in the laser workstation for a laser beam with a wavelength of 1040 nm and a frequency of 100 kHz. (blue) internal power of the laser system itself. (orange) output power of the laser beam without an focusing objective in place. (yellow) output power under a 2,5x objective.

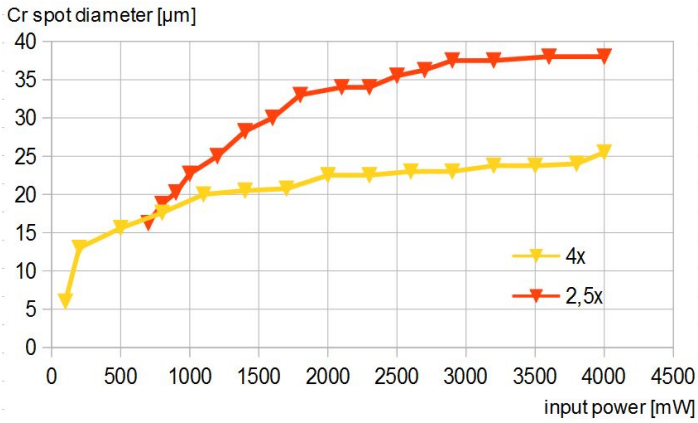

Fig. 9.7: Spot size of the focused laser beam in a chromium layer of 250 nm produced of a single pulse through an objective with (orange) 2,5x and (yellow) 4x magnification.

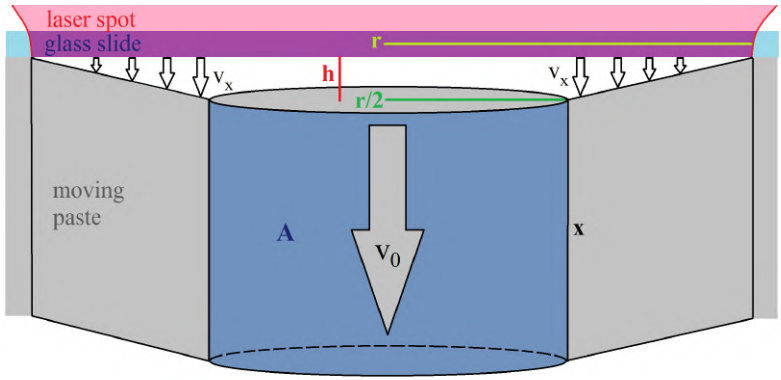

Fig. 9.8: Schematic for the estimations of the force necessary to bend the layer F_{bend}.

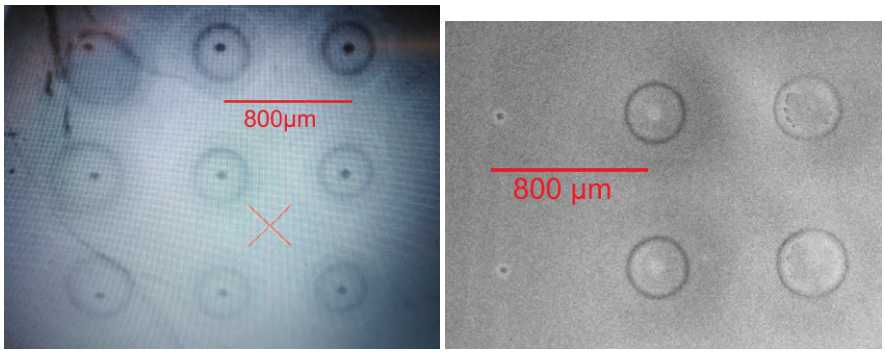

Fig. 9.9: Effect of the gas bubble in nanopaste imaged (left) in the laser work station and (right) with a light microscope. The both dots in the left of the right image show explosion transfers. All other circles are droplet transfers.